

The James Webb Space Telescope Mission

JONATHAN P. GARDNER,¹ JOHN C. MATHER,¹ RANDY ABBOTT,^{2,3} JAMES S. ABELL,¹ MARK ABERNATHY,⁴
FAITH E. ABNEY,⁴ JOHN G. ABRAHAM,¹ ROBERTO ABRAHAM,^{5,6} YASIN M. ABUL-HUDA,⁴ SCOTT ACTON,²
CYNTHIA K. ADAMS,¹ EVAN ADAMS,⁴ DAVID S. ADLER,⁴ MAARTEN ADRIAENSEN,⁷ JONATHAN ALBERT AGUILAR,⁴
MANSOOR AHMED,^{1,3} NASIF S. AHMED,⁴ TANJIRA AHMED,¹ RÜDEGER ALBAT,⁷ LOÏC ALBERT,⁸ STACEY ALBERTS,⁹
DAVID ALDRIDGE,¹⁰ MARY MARSHA ALLEN,⁴ SHAUNE S. ALLEN,¹ MARTIN ALTENBURG,¹¹ SERHAT ALTUNC,¹
JOSE LORENZO ALVAREZ,¹² JAVIER ÁLVAREZ-MÁRQUEZ,¹³ CATARINA ALVES DE OLIVEIRA,¹⁴ LESLIE L. AMBROSE,¹
SATYA M. ANANDAKRISHNAN,¹⁵ GREGORY C. ANDERSEN,¹ HARRY JAMES ANDERSON,⁴ JAY ANDERSON,⁴
KRISTEN ANDERSON,¹⁵ SARA M. ANDERSON,⁴ JULIO APREA,⁷ BENITA J. ARCHER,¹ JONATHAN W. ARENBERG,¹⁵
IOANNIS ARGYRIOU,¹⁶ SANTIAGO ARRIBAS,¹³ ÉTIENNE ARTIGAU,⁸ AMANDA ROSE ARVAI,⁴ PAUL ATCHESON,^{2,3}
CHARLES B. ATKINSON,¹⁵ JESSE AVERBUKH,⁴ CAGATAY AYMERGEN,¹ JOHN J. BACINSKI,⁴ WAYNE E. BAGGETT,⁴
GIORGIO BAGNASCO,¹² LYNN L. BAKER,¹ VICKI ANN BALZANO,⁴ KIMBERLY A. BANKS,¹ DAVID A. BARAN,¹
ELIZABETH A. BARKER,⁴ LARRY K. BARRETT,¹ BRUCE O. BARRINGER,⁴ ALLISON BARTO,² WILLIAM BAST,⁴
PIERRE BAUDOZ,¹⁷ STEFI BAUM,¹⁸ THOMAS G. BEATTY,¹⁹ MATHILDE BEAULIEU,²⁰ KATHRYN BECHTOLD,⁴ TRACY BECK,⁴
MEGAN M. BEDDARD,⁴ CHARLES BEICHMAN,²¹ LARRY BELLAGAMA,¹⁵ PIERRE BELY,^{4,3} TIMOTHY W. BERGER,¹⁵
LOUIS E. BERGERON,⁴ ANTOINE DARVEAU-BERNIER,⁸ MARIA D. BERTCH,⁴ CHARLOTTE BESKOW,⁷ LAURA E. BETZ,¹
CARL P. BIAGETTI,⁴ STEPHAN BIRKMANN,²² KURT F. BJORKLUND,¹⁵ JAMES D. BLACKWOOD,¹ RONALD PAUL BLAZEK,⁴
STEPHEN BLOSSFELD,¹⁵ MARCEL BLUTH,²³ ANTHONY BOCCALETTI,¹⁷ MARTIN E. BOEGNER JR.,⁴ RALPH C. BOHLIN,⁴
JOHN JOSEPH BOIA,⁴ TORSTEN BÖKER,²² N. BONAVENTURA,²⁴ NICHOLAS A. BOND,^{1,25} KARI ANN BOSLEY,⁴
RENE A. BOUCARUT,¹ PATRICE BOUCHET,²⁶ JEROEN BOUWMAN,²⁷ GARY BOWER,⁴ ARIEL S. BOWERS,⁴
CHARLES W. BOWERS,¹ LESLYE A. BOYCE,¹ CHRISTINE T. BOYER,⁴ MARTHA L. BOYER,⁴ MICHAEL BOYER,⁴
ROBERT BOYER,⁴ LARRY D. BRADLEY,⁴ GREGORY R. BRADY,⁴ BERNHARD R. BRANDL,²⁸ JUDITH L. BRANNEN,¹
DAVID BREDI,²⁹ HAROLD G. BREMMER,^{1,3} DAVID BRENNAN,⁴ PAMELA A. BRESNAHAN,⁴ STACEY N. BRIGHT,⁴
BRIAN J. BROILES,¹ ASA BROMENSCHENKEL,⁴ BRIAN H. BROOKS,⁴ KEIRA J. BROOKS,⁴ BOB BROWN,^{2,3} BRUCE BROWN,¹⁵
THOMAS M. BROWN,⁴ BARRY W. BRUCE,^{1,3} JONATHAN G. BRYSON,¹ EDWIN D. BUJANDA,¹⁵ BLAKE M. BULLOCK,¹⁵
A. J. BUNKER,³⁰ RAFAEL BUREO,¹² IRVING J. BURT,¹ JAMES AARON BUSH,⁴ HOWARD A. BUSHOUSE,⁴
MARIE C. BUSSMAN,¹ OLIVIER CABAUD,⁷ STEVEN CALE,¹ CHARLES D. CALHOON,¹ HUMBERTO CALVANI,⁴
ALICIA M. CANIPE,⁴ FRANCIS M. CAPUTO,⁴ MIHAI CARA,⁴ LARKIN CAREY,² MICHAEL ELI CASE,⁴ THADDEUS CESARI,¹
LEE D. CETORELLI,^{1,3} DON R. CHANCE,⁴ LYNN CHANDLER,¹ DAVE CHANEY,² GEORGE N. CHAPMAN,⁴ S. CHARLOT,³¹
PIERRE CHAYER,⁴ JEFFREY I. CHEEZUM,¹⁵ BIN CHEN,⁴ CHRISTINE H. CHEN,⁴ BRIAN CHERINKA,⁴ SARAH C. CHICHESTER,⁴
ZACHARY S. CHILTON,⁴ DHARINI CHITTIRAI BALAN,⁴ MARK CLAMPIN,³² CHARLES R. CLARK,¹ KERRY W. CLARK,⁴
STEPHANIE M. CLARK,¹ EDWARD E. CLAYBROOKS,¹ KEITH A. CLEVELAND,¹ ANDREW L. COHEN,¹⁵ LESTER M. COHEN,³³
KNICOLE D. COLÓN,¹ BENEE L. COLEMAN,⁴ LUIS COLINA,¹³ BRIAN J. COMBER,¹ THOMAS M. COMEAU,⁴ THOMAS COMER,⁴
ALAIN CONDE REIS,⁷ DENNIS C. CONNOLLY,¹ KYLE E. CONROY,⁴ ADAM R. CONTOS,^{2,34} JAMES CONTRERAS,²
NEIL J. COOK,⁸ JAMES L. COOPER,¹ RACHEL AVIVA COOPER,⁴ MICHAEL F. CORREIA,¹ MATTEO CORRENTI,⁴
CHRISTOPHE COSSOU,³⁵ BRIAN F. COSTANZA,¹⁵ ALAIN COULAIS,³⁶ COLIN R. COX,⁴ RAY T. COYLE,¹⁵
MISTY M. CRACRAFT,⁴ ALBERTO NORIEGA-CRESPO,⁴ KEITH A. CREW,⁴ GARY J. CURTIS,⁴ BIANCA CUSVELLER,¹²
CLEYCIANE DA COSTA MACIEL,³⁷ CHRISTOPHER T. DAILEY,¹ FRÉDÉRIC DAUGERON,⁷ GREG S. DAVIDSON,¹⁵
JAMES E. DAVIES,⁴ KATHERINE ANNE DAVIS,⁴ MICHAEL S. DAVIS,¹ RATNA DAY,¹ DANIEL DE CHAMBURE,^{37,7}
PAULINE DE JONG,^{12,3} GUIDO DE MARCHI,¹² BRUCE H. DEAN,¹ JOHN E. DECKER,^{1,3} AMY S. DELISA,¹
LAWRENCE C. DELL,¹ GAIL DELLAGATTA,^{1,3} FRANCISZKA DEMBINSKA,⁷ SANDOR DEMOSTHENES,²
NADEZHDA M. DENCHEVA,⁴ PHILIPPE DENEU,³⁸ WILLIAM W. DEPRIEST,⁴ JEREMY DESCHENES,⁴ NATHALIE DETHIENNE,³⁸
ÖRS HUNOR DETRE,²⁷ ROSA IZELA DIAZ,⁴ DANIEL DICKEN,³⁹ AUDREY S. DIFELICE,⁴ MATTHEW DILLMAN,⁴
MAUREEN O. DISHAROON,¹ EWINE F. VAN DISHOECK,²⁸ WILLIAM V. DIXON,⁴ JESSE B. DOGGETT,⁴
KEISHA L. DOMINGUEZ,¹ THOMAS S. DONALDSON,⁴ CRISTINA M. DORIA-WARNER,¹ TONY DOS SANTOS,³⁷
HEATHER DOTY,² ROBERT E. DOUGLAS, JR.,⁴ RENÉ DOYON,⁸ ALAN DRESSLER,⁴⁰ JENNIFER DRIGGERS,¹
PHILLIP A. DRIGGERS,¹ JAMIE L. DUNN,¹ KIMBERLY C. DUPRIE,⁴ JEAN DUPUIS,⁴¹ JOHN DURNING,^{1,3}
SANGHAMITRA B. DUTTA,³² NICHOLAS M. EARL,⁴ PAUL ECCLESTON,⁴² PASCAL ECOBICHON,³⁸ EIICHI EGAMI,⁹
RALF EHRENWINKLER,¹¹ JONATHAN D. EISENHAMER,⁴ MICHAEL EISENHOWER,³³ DANIEL J. EISENSTEIN,³³
ZAKY EL HAMEL,¹² MICHELLE L. ELIE,⁴ JAMES ELLIOTT,⁴ KYLE WESLEY ELLIOTT,⁴ MICHAEL EGRESSER,⁴
NÉSTOR ESPINOZA,⁴ ODESSA ETIENNE,⁴ MIREYA ETXALUZE,⁴² LEAH EVANS,⁴ LUCE FABREGUETTES,⁷ MASSIMO FALCOLINI,¹²
PATRICK R. FALINI,⁴ CURTIS FATIG,^{1,3} MATTHEW FEENEY,⁴ LEE D. FEINBERG,¹ RAYMOND FELS,¹² NAZMA FERDOUS,⁴
HENRY C. FERGUSON,⁴ LAURA FERRARESE,⁴³ MARIE-HÉLÈNE FERREIRA,³⁷ PIERRE FERRUIT,^{14,12} MALCOLM FERRY,⁴⁴

JOSEPH CHARLES FILIPPAZZO,⁴ DANIEL FIRRE,⁴⁵ MEES FIX,⁴ NICOLAS FLAGEY,⁴ KATHRYN A. FLANAGAN,⁴
 SCOTT W. FLEMING,⁴ MICHAEL FLORIAN,⁹ JAMES R. FLYNN,¹⁵ LUCA FOIADELLI,⁴⁵ MARK R. FONTAINE,^{1,3}
 ERIN MARIE FONTANELLA,⁴ PETER RANDOLPH FORSHAY,⁴ ELIZABETH A. FORTNER,^{1,3} ORI D. FOX,⁴
 ALEXANDRO P. FRAMARINI,⁴ JOHN I. FRANCISCO,¹⁵ RANDY FRANCK,² MARIJN FRANX,²⁸ DAVID E. FRANZ,¹
 SCOTT D. FRIEDMAN,⁴ KATHERYN E. FRIEND,¹⁵ JAMES R. FROST,¹ HENRY FU,¹⁵ ALEXANDER W. FULLERTON,⁴
 LIONEL GAILLARD,¹² SERGEY GALKIN,⁴ BEN GALLAGHER,^{2,46} ANTHONY D. GALYER,¹ MACARENA GARCÍA MARÍN,²²
 LISA E. GARDNER,⁴ DENNIS GARLAND,⁴ BRUCE ALBERT GARRETT,⁴ DANNY GASMAN,¹⁶ ANDRÁS GÁSPÁR,⁹
 RENÉ GASTAUD,²⁶ DANIEL GAUDREAU,⁴¹ PETER TIMOTHY GAUTHIER,⁴ VINCENT GEERS,³⁹ PAUL H. GEITHNER,¹
 MARIO GENNARO,⁴ JOHN GERBER,^{2,3} JOHN C. GEREAU,¹⁵ ROBERT GIAMPAOLI,¹⁵ GIOVANNA GIARDINO,²²
 PAUL C. GIBBONS,¹ KAROLINA GILBERT,⁴ LARRY GILMAN,¹⁵ JULIEN H. GIRARD,⁴ MARK E. GIULIANO,⁴
 KONSTANTINOS GKOUNTIS,⁷ ALISTAIR GLASSE,³⁹ KIRK ZACHARY GLASSMIRE,⁴ ADRIAN MICHAEL GLAUSER,⁴⁷
 STUART D. GLAZER,¹ JOSHUA GOLDBERG,⁴ DAVID A. GOLIMOWSKI,⁴ SHIREEN P. GONZAGA,⁴ KARL D. GORDON,⁴
 SHAWN J. GORDON,¹⁵ PAUL GOUDFROOIJ,⁴ MICHAEL J. GOUGH,⁴ ADRIAN J. GRAHAM,¹² CHRISTOPHER M. GRAU,¹
 JOEL DAVID GREEN,⁴ GRETCHEN R. GREENE,⁴ THOMAS P. GREENE,⁴⁸ PERRY E. GREENFIELD,⁴
 MATTHEW A. GREENHOUSE,¹ THOMAS R. GREVE,⁴⁹ EDGAR M. GREVILLE,¹ STEFANO GRIMALDI,² FRANK E. GROE,¹⁵
 ANDREW GROEBNER,⁴ DAVID M. GRUMM,⁴ TIMOTHY GRUNDY,⁴² MANUEL GÜDEL,⁴ PIERRE GUILLARD,³¹
 JOHN GULDALIAN,¹⁵ CHRISTOPHER A. GUNN,¹ ANTHONY GURULE,² IRVIN MEYER GUTMAN,⁴ PAUL D. GUY,^{1,51}
 BENJAMIN GUYOT,⁷ WARREN J. HACK,⁴ PETER HADERLEIN,²⁹ JAMES B. HAGAN,⁴ ANDRIA HAGEDORN,¹⁵ KEVIN HAINLINE,⁹
 CRAIG HALEY,¹⁰ MARYAM HAMI,⁴ FORREST CLIFFORD HAMILTON,⁴ JEFFREY HAMMANN,¹⁵ HEIDI B. HAMMEL,⁵²
 CHRISTOPHER J. HANLEY,⁴ CARL AUGUST HANSEN,⁴ BRUCE HARDY,^{2,3} BERND HARNISCH,^{12,3} MICHAEL HUNTER HARR,⁴
 PAMELA HARRIS,¹ JESSICA ANN HART,⁴ GEORGE F. HARTIG,⁴ HASHIMA HASAN,³² KATHLEEN MARIE HASHIM,⁴
 RYAN HASHIMOTO,¹⁵ SUJEE J. HASKINS,¹ ROBERT EDWARD HAWKINS,^{4,51} BRIAN HAYDEN,⁴ WILLIAM L. HAYDEN,^{1,3}
 MIKE HEALY,¹² KAREN HECHT,⁴ VINCE J. HEEG,¹⁵ REEM HEJAL,¹⁵ KRISTOPHER A. HELM,⁴ NICHOLAS J. HENGEMHLE,¹
 THOMAS HENNING,²⁷ ALAINA HENRY,⁴ RONALD L. HENRY,⁴ KATHERINE HENSHAW,⁴ SCARLIN HERNANDEZ,⁴
 DONALD C. HERRINGTON,⁴ ASTRID HESKE,¹² BRIGETTE EMILY HESMAN,⁴ DAVID L. HICKEY,⁴ BRYAN N. HILBERT,⁴
 DEAN C. HINES,⁴ MICHAEL R. HINZ,¹⁵ MICHAEL HIRSCH,¹⁵ ROBERT S. HITCHO,⁴ KLAUS HODAPP,⁵³ PHILIP E. HODGE,⁴
 MELISSA HOFFMAN,⁴ SHERIE T. HOLFELTZ,⁴ BRYAN JASON HOLLER,⁴ JENNIFER ROSE HOPPA,⁴ SCOTT HORNER,⁴⁸
 JOSEPH M. HOWARD,¹ RICHARD J. HOWARD,^{32,3} JEAN M. HUBER,¹ JOSEPH S. HUNKELER,⁴ ALEXANDER HUNTER,⁴
 DAVID GAVIN HUNTER,⁴ SPENCER W. HURD,¹ BRENDAN J. HURST,⁴ JOHN B. HUTCHINGS,⁴³ JASON E. HYLAN,¹
 LUMINITA ILINCA IGNAT,⁴¹ GARTH ILLINGWORTH,⁵⁴ SANDRA M. IRISH,¹ JOHN C. ISAACS III,⁴ WALLACE C. JACKSON JR.,¹⁵
 DANIEL T. JAFFE,⁵⁵ JASMIN JAHIC,¹⁵ AMIR JAHROMI,¹ PETER JAKOBSEN,²⁴ BRYAN JAMES,¹ JOHN C. JAMES,¹
 LEANDREA RAE JAMES,⁴ WILLIAM BRIAN JAMESON,⁴ RAYMOND D. JANDRA,¹⁵ RAY JAYAWARDHANA,⁵⁶
 ROBERT JEDRZEJEWSKI,⁴ BASIL S. JEFFERS,¹ PETER JENSEN,¹² EGGES JOANNE,^{2,3} ALAN T. JOHNS,¹ CARL A. JOHNSON,⁴
 ERIC L. JOHNSON,¹ PATRICIA JOHNSON,^{1,3} PHILLIP STEPHEN JOHNSON,⁴ THOMAS K. JOHNSON,¹ TIMOTHY W. JOHNSON,⁴
 DOUG JOHNSTONE,^{43,57} DELPHINE JOLLET,¹² DANNY P. JONES,⁴ GREGORY S. JONES,¹⁵ OLIVIA C. JONES,³⁹
 RONALD A. JONES,¹ VICKI JONES,⁴ IAN J. JORDAN,⁴ MARGARET E. JORDAN,⁴ REGINALD JUE,¹⁵ MARK H. JURKOWSKI,¹
 GRANT JUSTIS,⁴ KAY JUSTANONT,⁵⁸ CATHERINE C. KALEIDA,⁴ JASON S. KALIRAI,⁵⁹ PHILLIP CABRALES KALMANSON,⁴
 LISA KALTENEGGER,⁵⁶ JENS KAMMERER,⁴ SAMUEL K. KAN,¹⁵ GRAHAM CHILDS KANAREK,⁴ SHAW-HONG KAO,⁴
 DIANE M. KARAKLA,⁴ HERMANN KARL,¹¹ SUSAN A. KASSIN,^{4,60} DAVID D. KAUFFMAN,⁴ PATRICK KAVANAGH,⁶¹
 LEIGH L. KELLEY,¹ DOUGLAS M. KELLY,⁹ SARAH KENDREW,²² HERBERT V. KENNEDY,⁴ DEBORAH A. KENNY,⁴
 RITVA A. KESKI-KUHA,¹ CHARLES D. KEYES,⁴ ALI KHAN,¹² RICHARD C. KIDWELL,⁴ RANDY A. KIMBLE,¹
 JAMES S. KING,^{1,3} RICHARD C. KING,¹ WAYNE M. KINZEL,⁴ JEFFREY R. KIRK,¹ MARC E. KIRKPATRICK,¹⁵
 PAMELA KLAASSEN,³⁹ LANA KLINGEMANN,² PAUL U. KLINTWORTH,¹⁵ BRYAN ADAM KNAPP,⁴ SCOTT KNIGHT,²
 PERRY J. KNOLLENBERG,¹⁵ DANIEL MARK KNUTSEN,⁴ ROBERT KOEHLER,⁴ ANTON M. KOEKEMOER,⁴ EARL T. KOFLER,¹⁵
 VICKI L. KONTSON,¹ AIDEN ROSE KOVACS,⁴ VERA KOZHURINA-PLATAIS,⁴ OLIVER KRAUSE,²⁷ GERARD A. KRISS,⁴
 JOHN KRIST,²⁹ MONICA R. KRISTOFFERSEN,¹⁵ CLAUDIA KROGEL,¹ ANTHONY P. KRUEGER,⁴ BERNARD A. KULP,⁴
 NIMISHA KUMARI,²² SANDY W. KWAN,²⁹ MARK KYPRIANOU,⁴ AURORA GADIANO LABADOR,⁴ ÁLVARO LABIANO,⁶²
 DAVID LAFRENIÈRE,⁸ PIERRE-OLIVIER LAGAGE,³⁵ VICTORIA G. LAIDLER,⁴ BENOIT LAINE,¹² SIMON LAIRD,¹²
 CHARLES-PHILIPPE LAJOIE,⁴ MATTHEW D. LALLO,⁴ MAY YEN LAM,⁴ STEPHANIE MARIE LAMASSA,⁴ SCOTT D. LAMBROS,¹
 RICHARD JOSEPH LAMPENFIELD,⁴ MATTHEW ED LANDER,¹ JAMES HUTTON LANGSTON,⁴ KIRSTEN LARSON,²²
 MELORA LARSON,²⁹ ROBERT JOSEPH LAVERGHETTA,⁴ DAVID R. LAW,⁴ JON F. LAWRENCE,¹ DAVID W. LEE,¹⁵
 JANICE LEE,^{4,63,9} YAT-NING PAUL LEE,⁴ JARRON LEISENRING,⁹ MICHAEL DUNLAP LEVEILLE,⁴ NANCY A. LEVENSON,⁴
 JOSHUA S. LEVI,¹⁵ MARIE B. LEVINE,²⁹ DAN LEWIS,⁴⁴ JAKE LEWIS,^{2,64} NIKOLE LEWIS,⁵⁶ MATTIA LIBRALATO,²²
 NORBERT LIDON,³⁸ PAULA LOUISA LIEBRECHT,⁴ PAUL LIGHTSEY,^{2,3} SIMON LILLY,⁴⁷ FREDERICK C. LIM,¹ PEY LIAN LIM,⁴
 SAI-KWONG LING,¹⁵ LISA J. LINK,¹ MIRANDA NICOLE LINK,⁴ JAMIE L. LIPINSKI,⁴ XIAOLI LIU,⁴ AMY S. LO,¹⁵
 LYNETTE LOBMEYER,² RYAN M. LOGUE,⁴ CHRIS A. LONG,⁴ DOUGLAS R. LONG,⁴ ILANA D. LONG,⁴ KNOX S. LONG,⁴
 MARCOS LÓPEZ-CANIEGO,⁶⁵ JENNIFER M. LOTZ,⁴ JENNIFER M. LOVE-PRUITT,¹⁵ MICHAEL LUBSKIY,⁴ EDWARD B. LUERS,^{1,3}
 ROBERT A. LUETGENS,¹⁵ ANNETTA J. LUEVANO,¹⁵ SARAH MARIE G. FLORES LUI,⁴ JAMES M. LUND III,¹⁵
 RAY A. LUNDQUIST,³² JONATHAN LUNINE,⁵⁶ NORA LÜTZGENDORF,²² RICHARD J. LYNCH,^{1,66} ALEX J. MACDONALD,⁴
 KENNETH MACDONALD,⁴ MATTHEW J. MACIAS,¹⁵ KEITH I. MACKLIS,¹⁵ PEIMAN MAGHAMI,¹ RISHABH Y. MAHARAJA,¹
 ROBERTO MAIOLINO,^{67,68} KONSTANTINOS G. MAKRYGIANNIS,¹⁵ SUNITA GIRI MALLA,⁴ ELIOT M. MALUMUTH,¹
 ELENA MANJAVACAS,²² ANDREA MARINI,¹² AMANDA MARRIONE,⁴ ANTHONY MARSTON,¹⁴ ANDRÉ R. MARTEL,⁴

DIDIER MARTIN,¹² PETER G. MARTIN,⁶⁹ KRISTIN L. MARTINEZ,² MARC MASCHMANN,¹¹ GREGORY L. MASCI,⁴
 MARGARET E. MASETTI,^{1,25} MICHAEL MASZKIEWICZ,⁴¹ GARY MATTHEWS,¹ JACOB E. MATUSKEY,⁴ GLEN A. MCBRAYNER,¹⁵
 DONALD W. MCCARTHY,⁹ MARK J. MCCAUGHREAN,¹² LESLIE A. MCCLARE,¹ MICHAEL D. MCCLARE,¹
 JOHN C. MCCLOSKEY,¹ TAYLORE D. MCCLURG,¹⁵ MARTIN MCCOY,¹ MICHAEL W. MCELWAIN,¹ ROY D. MCGREGOR,¹⁵
 DOUGLAS B. MCGUFFEY,¹ ANDREW G. MCKAY,¹⁵ WILLIAM K. MCKENZIE,¹ BRIAN MCLEAN,⁴ MATTHEW MCMASTER,⁴
 WARREN MCNEIL,^{1,3} WIM DE MEESTER,¹⁶ KIMBERLY L. MEHALICK,¹ MARGARET MEIXNER,⁴ MARCIO MELÉNDEZ,⁴
 MICHAEL P. MENZEL,¹ MICHAEL T. MENZEL,¹ MATTHEW MERZ,⁴ DAVID D. MESTERHARM,¹ MICHAEL R. MEYER,⁷⁰
 MICHELE L. MEYETT,⁴ LUIS E. MEZA,¹⁵ CALVIN MIDWINTER,¹⁰ STEFANIE N. MILAM,¹ JAY TODD MILLER,⁴
 WILLIAM C. MILLER,¹ CHERIE L. MISKEY,¹ KARL MISSELT,⁹ EILEEN P. MITCHELL,¹ MARTIN MOHAN,¹⁵
 EMILY E. MONTOYA,¹ MICHAEL J. MORAN,¹⁵ TAKAHIRO MORISHITA,⁴ AMAYA MORO-MARTÍN,⁴ DEBRA L. MORRISON,⁴
 JANE MORRISON,⁹ ERNIE C. MORSE,⁴ MICHAEL MOSCHOS,¹⁵ S. H. MOSELEY,^{71,1} GARY E. MOSIER,¹ PETER MOSNER,¹¹
 MATT MOUNTAIN,⁵² JASON S. MUCKENTHALER,¹⁵ DONALD G. MUELLER,⁴ MIGO MUELLER,⁷² DANIELLA MUHIEM,^{1,51}
 PRISCA MÜHLMANN,¹² SUSAN ELIZABETH MULLALLY,⁴ STEPHANIE M. MULLEN,¹ ALAN J MUNGER,¹⁵ JESS MURPHY,²
 KATHERINE T. MURRAY,⁴ JAMES C. MUZEROLLE,⁴ MATTHEW MYCROFT,²⁹ ANDREW MYERS,⁴ CAREY R. MYERS,⁴
 FRED RICHARD R. MYERS,¹⁵ RICHARD MYERS,¹⁵ KAILA MYRICK,⁴ ADRIAN F. NAGLE, IV,² OMNARAYANI NAYAK,⁴
 BRET NAYLOR,²⁹ SUSAN G. NEFF,¹ EDMUND P. NELAN,⁴ JOHN NELLA,¹⁵ DUY TUONG NGUYEN,⁴ MICHAEL N. NGUYEN,¹
 BRYONY NICKSON,⁴ JOHN JOSEPH NIDHIRY,⁴ MALCOLM B. NIEDNER,^{1,3} MARIA NIETO-SANTISTEBAN,⁴
 NIKOLAY K. NIKOLOV,⁴ MARY ANN NISHISAKA,¹⁵ ALBERTO NORIEGA-CRESPO,⁴ ANTONELLA NOTA,^{22,3}
 ROBYN C. O'MARA,¹ MICHAEL OBORYSHKO,⁴ MARCUS B. O'BRIEN,¹⁵ WILLIAM R. OCHS,^{1,3} JOEL D. OFFENBERG,^{73,74}
 PATRICK MICHAEL OGLE,⁴ RAYMOND G. OHL,¹ JOSEPH HAMDEN OLMSTED,⁴ SHANNON BARBARA OSBORNE,⁴
 BRIAN PATRICK O'SHAUGHNESSY,⁴ GÖRAN ÖSTLIN,⁷⁵ BRIAN O'SULLIVAN,²² O. JUSTIN OTOR,⁴ RICHARD OTTENS,¹
 NATHALIE N.-Q. OUELLETTE,⁸ DARIA J. OUTLAW,¹ BEVERLY A. OWENS,⁴ CAMILLA PACIFICI,⁴ JAMES CHRISTOPHE PAGE,⁴
 JAMES G. PARANILAM,⁴ SANG PARK,³³ KEITH A. PARRISH,¹ LAURA PASCHAL,¹ POLYCHRONIS PATAPIS,⁴⁷ JIGNASHA PATEL,¹
 KEITH PATRICK,¹⁵ ROBERT A. PATTISHALL JR.,¹⁵ DOUGLAS WILLIAM PAUL,⁴ SHIRLEY J. PAUL,¹ TYLER ANDREW PAULY,⁴
 CHERYL M. PAVLOVSKY,⁴ MARIA PEÑA-GUERRERO,⁴ ANDREW H. PEDDER,⁴ MATTHEW WELDON PEEK,⁴
 PATRICIA A. PELHAM,⁴ KONSTANTIN PENANEN,²⁹ BETH A. PERRIELLO,⁴ MARSHALL D. PERRIN,⁴ RICHARD F. PERRINE,⁴
 CHUCK PERRYGO,^{1,3} MURIEL PESLIER,³⁷ MICHAEL PETACH,¹⁵ KARLA A. PETERSON,⁴ TOM PFARR,^{1,3} JAMES M. PIERSON,¹
 MARTIN PIETRASZKIEWICZ,¹⁵ GUY PILCHEN,⁷ JUDY L. PIPHER,⁷⁶ NORBERT PIRZKAL,²² JOSEPH T. PITMAN,¹
 DANIELLE M. PLAYER,¹⁵ RACHEL PLESHA,⁴ ANJA PLITZKE,¹² JOHN A. POHNER,¹⁵ KARYN KONSTANTIN POLETIS,⁴
 JOSEPH A. POLLIZZI,⁴ ETHAN POLSTER,⁴ JAMES T. PONTIUS,¹ KLAUS PONTOPPIDAN,⁴ SUSANA C. PORGES,¹⁵
 GREGG D. POTTER,¹⁵ STEPHEN PRESCOTT,⁴ CHARLES R. PROFFITT,⁴ LAURENT PUEYO,⁴ IRMA ARACELY QUISPE NEIRA,⁴
 ARMANDO RADICH,^{1,3} REIKO T. RAGER,⁴ JULIEN RAMEAU,^{8,77} DEBORAH D. RAMEY,^{1,51} RAFAEL RAMOS ALARCON,⁴
 RICCARDO RAMPINI,¹² ROBERT RAPP,¹ ROBERT A. RASHFORD,¹ BERNARD J. RAUSCHER,¹ SWARA RAVINDRANATH,⁴
 TIMOTHY RAWLE,²² TYNIKA N. RAWLINGS,¹ TOM RAY,⁶¹ MICHAEL W. REGAN,⁴ BRIAN REHM,^{1,3} KENNETH D. REHM,⁷⁸
 NEILL REID,⁴ CARL A. REIS,¹ FLORIAN RENK,⁴⁵ TOM B. REOCH,¹⁵ MICHAEL RESSLER,²⁹ ARMIN W. REST,⁴
 PAUL J. REYNOLDS,¹⁵ JOEL G. RICHON,⁴ KAREN V. RICHON,¹ MICHAEL RIDGAWAY,⁴ ADRIAN RICHARD RIEDEL,⁴
 GEORGE H. RIEKE,⁹ MARCIA J. RIEKE,⁹ RICHARD E. RIFELLI,¹⁵ JANE R. RIGBY,¹ CATHERINE S. RIGGS,⁴
 NANCY J. RINGEL,¹ CHRISTINE E. RITCHIE,⁴ HANS-WALTER RIX,²⁷ MASSIMO ROBERTO,^{4,60} MICHAEL S. ROBINSON,⁴
 ORION ROBINSON,⁴ FRANK W. ROCK,⁴ DAVID R. RODRIGUEZ,⁴ BRUNO RODRÍGUEZ DEL PINO,¹³ THOMAS ROELLIG,⁴⁸
 SCOTT O. ROHRBACH,¹ ANTHONY J. ROMAN,⁴ FREDERICK J. ROMELFANGER,⁴ FELIPE P. ROMO JR.,¹ JOSE J. ROSALES,¹
 PERRY ROSE,⁴ ANTHONY F. ROTELIUK,¹⁵ MARC N. ROTH,¹⁵ BRADEN QUINN ROTHWELL,⁴ SYLVAIN ROUZAUD,³⁸
 JASON ROWE,⁷⁹ NEIL ROWLANDS,¹⁰ ARPITA ROY,⁴ PIERRE ROYER,¹⁶ CHUNLEI RUI,¹⁵ PETER RUMLER,^{12,3}
 WILLIAM RUMPL,⁴ MELISSA L. RUSS,⁴ MICHAEL B. RYAN,¹⁵ RICHARD M. RYAN,³² KARL SAAD,⁴¹ MODHUMITA SABATA,⁴
 RICK SABATINO,¹ ELENA SABBBI,⁴ PHILLIP A. SABELHAUS,^{1,51} STEPHEN SABIA,¹ KAILASH C. SAHU,⁴ BABAK N. SAIF,^{1,4}
 JEAN-CHRISTOPHE SALVIGNOL,¹² PIYAL SAMARA-RATNA,⁸⁰ BRIDGET S. SAMUELSON,¹⁵ FELICIA A. SANDERS,²⁹
 BRADLEY SAPPINGTON,⁴ B. A. SARGENT,^{4,60} ARNE SAUER,¹¹ BRUCE J. SAVADKIN,^{1,3} MARCIN SAWICKI,⁸¹
 TINA M. SCHAPELL,¹ CAROLINE SCHEFFER,¹² SILVIA SCHEITHAUER,²⁷ RON SCHERER,¹⁵ CONRAD SCHIFF,¹
 EVERETT SCHLAWIN,⁹ OLIVIER SCHMEITZKY,¹² TYLER S. SCHMITZ,⁴ DONALD J. SCHMUDE,¹⁵ ANALYN SCHNEIDER,²⁹
 JÜRGEN SCHREIBER,²⁷ HILDE SCHROEVEN-DECEUNINCK,¹² JOHN J. SCHULTZ,⁴ RYAN SCHWAB,⁴ CURTIS H. SCHWARTZ,¹
 DARIO SCOCCIMARRO,⁷ JOHN F. SCOTT,⁴ MICHELLE B. SCOTT,¹ BONITA L. SEATON,¹ BRUCE S. SEELY,⁴
 BERNARD SEERY,⁸² MARK SEIDLECK,^{1,3} KENNETH SEMBACH,⁴ CLARE ELIZABETH SHANAHAN,⁴ BRYAN SHAUGHNESSY,⁴²
 RICHARD A. SHAW,⁴ CHRISTOPHER MICHAEL SHAY,⁴ EVEN SHEEHAN,¹ KARTIK SHETH,³² HSIN-YI SHIH,⁴ IRENE SHIVAEI,⁹
 NOAH SIEGEL,² MATTHEW G. SIENKIEWICZ,⁴ DEBRA D. SIMMONS,¹⁵ BERNARD P. SIMON,⁴ MARCO SIRIANNI,²²
 ANAND SIVARAMAKRISHNAN,^{4,83,60} JEFFREY E. SLADE,¹ G. C. SLOAN,⁴ CHRISTINE E. SLOCUM,⁴ STEVEN E. SLOWINSKI,⁴
 CORBETT T. SMITH,³¹ ERIC P. SMITH,³² ERIN C. SMITH,¹ KOPY SMITH,² ROBERT SMITH,⁸⁴ STEPHANIE J. SMITH,⁴
 JOHN L. SMOLIK,¹⁵ DAVID R. SODERBLOM,⁴ SANGMO TONY SOHN,⁴ JEFF SOKOL,² GEORGE SONNEBORN,^{1,3}
 CHRISTOPHER D. SONTAG,⁴ PETER R. SOOY,¹ REMI SOUMMER,⁴ DANA M. SOUTHWOOD,¹⁵ KAY SPAIN,⁴ JOSEPH SPARMO,¹
 DAVID T. SPEER,¹ RICHARD SPENCER,⁴ JOSEPH D. SPROFERA,¹⁵ SCOTT S. STALLCUP,⁴ MARCIA K. STANLEY,¹
 JOHN A. STANSBERRY,⁴ CHRISTOPHER C. STARK,¹ CARL W. STARR,¹ DIANE Y. STASSI,¹ JANE A. STECK,¹
 CHRISTINE D. STEELEY,¹ MATTHEW A. STEPHENS,¹ RALPH J. STEPHENSON,¹⁵ ALPHONSO C. STEWART,¹
 MASSIMO STIAVELLI,⁴ HERVEY STOCKMAN JR.,^{4,3} PAOLO STRADA,¹² AMBER N. STRAUGHN,¹ SCOTT STREETMAN,²
 DAVID KENDAL STRICKLAND,⁴ JINGPING F. STROBELE,¹⁵ MARTIN STUHLINGER,¹⁴ JEFFREY EDWARD STYS,⁴ MIGUEL SUCH,¹²

KALYANI SUKHATME,²⁹ JOSEPH F. SULLIVAN,^{2,3} PAMELA C. SULLIVAN,¹ SANDRA M. SUMNER,¹ FENGWU SUN,⁹
 BENJAMIN DALE SUNNQUIST,⁴ DARYL ALLEN SWADE,⁴ MICHAEL S. SWAM,⁴ DIANE F. SWENTON,¹ ROBBY A. SWOISH,¹⁵
 OI IN TAM LITTEN,⁴ LASZLO TAMAS,³⁹ ANDREW TAO,¹⁵ DAVID K. TAYLOR,⁴ JOANNA M. TAYLOR,⁴ MAURICE TE PLATE,²²
 MASON VAN TEA,⁴ KELLY K. TEAGUE,⁴ RANDAL C. TELFER,⁴ TEA TEMIM,⁸⁵ SCOTT C. TEXTER,¹⁵
 DEEPASHRI G. THATTE,⁴ CHRISTOPHER LEE THOMPSON,⁴ LINDA M. THOMPSON,⁴ SHAUN R. THOMSON,¹
 HARLEY THRONSON,^{1,3} C. M. TIERNEY,¹⁵ TUOMO TIKKANEN,⁸⁰ LEE TINNIN,⁹ WILLIAM THOMAS TIPPET,⁴
 CONNOR WILLIAM TODD,⁴ HIEN D. TRAN,⁴ JOHN TRAUGER,²⁹ EDWIN GREGORIO TREJO,⁴ JUSTIN HOANG VINH TRUONG,⁴
 CHRISTINE L. TSUKAMOTO,¹⁵ YASIR TUFAIL,⁴ JASON TUMLINSON,⁴ SAMUEL TUSTAIN,⁴² HARRISON TYRA,⁴
 LEONARDO UBEDA,⁴ KELLI UNDERWOOD,⁴ MICHAEL A. UZZO,⁴ STEVEN VACLAVIK,⁴ FRIDA VALENDUC,³⁷ JEFF A. VALENTI,⁴
 JULIE VAN CAMPEN,¹ INGE VAN DE WETERING,¹² ROELAND P. VAN DER MAREL,⁴ REMY VAN HAARLEM,¹²
 BART VANDENBUSSCHE,¹⁶ DONA D. VANTERPOOL,¹ MICHAEL R. VERNON,¹⁵ MARIA BEGOÑA VILA COSTAS,^{1,23}
 KEVIN VOLK,⁴ PIET VOORZAAT,¹² MARK F. VOYTON,¹ EKATERINA VYDRA,⁴ DARRYL J. WADDY,¹
 CHRISTOFFEL WAELKENS,¹⁶ GLENN MICHAEL WAHLGREN,⁴ FREDERICK E. WALKER JR.,¹⁵ MICHEL WANDER,⁴¹
 CHRISTINE K. WARFIELD,⁴ GERALD WARNER,¹⁰ FRANCIS C. WASIAK,¹ MATTHEW F. WASIAK,¹ JAMES WEHNER,¹⁵
 KEVIN R. WEILER,¹⁵ MARK WEILERT,²⁹ STANLEY B. WEISS,¹⁵ MARTYN WELLS,³⁹ ALAN D. WELTY,⁴ LAUREN WHEATE,¹
 THOMAS P. WHEELER,⁴ CHRISTY L. WHITE,¹⁵ PAUL WHITEHOUSE,¹ JENNIFER MARGARET WHITELEATHER,⁴
 WILLIAM RUSSELL WHITMAN,⁴ CHRISTINA C. WILLIAMS,⁸⁶ CHRISTOPHER N. A. WILLMER,⁹ CHRIS J. WILLOTT,⁴³
 SCOTT P. WILLOUGHBY,¹⁵ ANDREW WILSON,¹⁰ DEBRA WILSON,⁹ DONNA V. WILSON,¹ ROGIER WINDHORST,⁸⁷
 EMILY CHRISTINE WISLOWSKI,⁴ DAVID J. WOLFE,⁴ MICHAEL A. WOLFE,⁴ SCHUYLER WOLFF,⁹ AMANCIO WONDEL,³⁷
 CINDY WOO,¹⁵ ROBERT T. WOODS,¹⁵ ELAINE WORDEN,^{2,3} WILLIAM WORKMAN,⁴ GILLIAN S. WRIGHT,³⁹ CARL WU,¹
 CHI-RAI WU,⁴ DAKIN D. WUN,¹⁵ KRISTEN B. WYMER,⁴ THOMAS YADETIE,⁴ ISABELLE C. YAN,¹ KEITH C. YANG,¹⁵
 KAYLA L. YATES,⁴ CHRISTOPHER R. YEAGER,⁴ ETHAN JOHN YERGER,⁴ ERICK T. YOUNG,⁸⁸ GARY YOUNG,¹⁵ GENE YU,¹⁵
 SUSAN YU,⁴ DEAN S. ZAK,⁴ PETER ZEIDLER,⁸⁹ ROBERT ZEPP,⁴ JULIA ZHOU,¹⁰ CHRISTIAN A. ZINCKE,¹ STEPHANIE ZONAK,⁴
 AND ELISABETH ZONDAG¹²

¹NASA Goddard Space Flight Center, 8800 Greenbelt Rd, Greenbelt, MD 20771, USA

²Ball Aerospace & Technologies Corp., 1600 Commerce Street, Boulder, CO 80301, USA

³Retired

⁴Space Telescope Science Institute, 3700 San Martin Drive, Baltimore, MD, 21218, USA

⁵Department of Astronomy & Astrophysics, University of Toronto, 50 St. George Street, Toronto, ON M5S 3H4, Canada

⁶Dunlap Institute for Astronomy and Astrophysics, University of Toronto, 50 St George Street, Toronto, ON M5S 3H4, Canada

⁷European Space Agency, HQ Daumesnil, 52 rue Jacques Hillairet, 75012 Paris, France

⁸Institut de Recherche sur les Exoplanètes (iREx), Université de Montréal, Département de Physique,
 C.P. 6128 Succ. Centre-ville, Montréal, QC H3C 3J7, Canada.

⁹Steward Observatory, University of Arizona, 933 N. Cherry Ave, Tucson, AZ 85721, USA

¹⁰Honeywell Aerospace #100, 303 Terry Fox Drive, Ottawa, ON K2K 3J1, Canada

¹¹Airbus Defence and Space GmbH, Ottobrunn, Germany

¹²European Space Agency, European Research & Technology Centre, Keplerlaan 1, Postbus 299, 2200 AG Noordwijk, The Netherlands

¹³Centro de Astrobiología (CAB, CSIC-INTA), Carretera de Ajalvir, E-28850 Torrejón de Ardoz, Madrid, Spain

¹⁴European Space Agency, European Space Astronomy Centre, Camino bajo del Castillo, s/n, Urbanización Villafranca del Castillo,
 28692 Villanueva de la Cañada, Madrid, Spain

¹⁵Northrop Grumman, One Space Park, Redondo Beach, CA 90278, USA

¹⁶Instituut voor Sterrenkunde, KU Leuven, Celestijnenlaan 200D, Bus-2410, 3000 Leuven, Belgium

¹⁷LESIA, Observatoire de Paris, Université PSL, CNRS, Sorbonne Université, Université de Paris, 5 place Jules Janssen, 92195
 Meudon, France

¹⁸Faculty of Science, 230 Machray Hall, 186 Dysart Road, University of Manitoba, Winnipeg, MB Canada R3T 2N2

¹⁹Department of Astronomy, University of Wisconsin, Madison, Madison, WI 53706

²⁰Université Côte d'Azur, Observatoire de la Côte d'Azur, CNRS, Laboratoire Lagrange, F-06108 Nice, France.

²¹NASA Exoplanet Science Institute/IPAC, Jet Propulsion Laboratory, California Institute of Technology, 1200 E California Blvd,
 Pasadena, CA 91125

²²European Space Agency, Space Telescope Science Institute, 3700 San Martin Drive, Baltimore, MD 21218, USA

²³KBR, 7701 Greenbelt Road, Greenbelt, MD 20770

²⁴Cosmic Dawn Center (DAWN), Niels Bohr Institute, University of Copenhagen, Jagtvej 128, DK-2200, Denmark

²⁵Adnet Systems, Inc., 6720B Rockledge Drive, Suite # 504, Bethesda, MD 20817, USA

²⁶Laboratoire AIM Paris-Saclay, CEA-IRFU/SaP, CNRS, Université Paris Diderot, F-91191 Gif-sur-Yvette, France

²⁷Max Planck Institute for Astronomy, Königstuhl 17, D-69117 Heidelberg, Germany

²⁸Leiden Observatory, Leiden University, PO Box 9513, 2300 RA Leiden, The Netherlands

²⁹Jet Propulsion Laboratory, California Institute of Technology, 4800 Oak Grove Dr., Pasadena, CA, 91109, USA

³⁰Department of Physics, University of Oxford, Denys Wilkinson Building, Keble Road, Oxford, OX1 3RH, UK

³¹Sorbonne Université, UPMC-CNRS, UMR7095, Institut d'Astrophysique de Paris, F-75014 Paris, France

- ³² NASA Headquarters, 300 E Street SW, Washington, DC 20546, USA
- ³³ The Center for Astrophysics, 60 Garden Street, Cambridge, MA 02138, USA
- ³⁴ Moog Space and Defense Group, 5025 N Robb St, Suite 500, Arvada, CO 80033, USA
- ³⁵ Université Paris-Saclay, Université de Paris, CEA, CNRS, AIM, F-91191 Gif-sur-Yvette, France
- ³⁶ LERMA (CNRS) & Observatoire de Paris, Paris, France
- ³⁷ European Space Agency, Centre Spatial Guyanais, BP816 – Route Nationale 1, 97388 Kourou CEDEX, French Guiana
- ³⁸ Centre national d'études spatiales, Direction des Lanceurs, 52 rue Jacques Hillairet, 75612 Paris CEDEX, France
- ³⁹ UK Astronomy Technology Centre, Royal Observatory Edinburgh, Blackford Hill, Edinburgh EH9 3HJ, UK
- ⁴⁰ The Observatories, The Carnegie Institution for Science, 813 Santa Barbara St., Pasadena, CA 91101, USA
- ⁴¹ Canadian Space Agency, 6767 Route de l'Aéroport, Saint-Hubert, QC J3Y 8Y9, Canada
- ⁴² RAL Space, STFC, Rutherford Appleton Laboratory, Harwell, Oxford, Didcot OX11 0QX, UK
- ⁴³ NRC Herzberg, 5071 West Saanich Rd, Victoria, BC V9E 2E7, Canada
- ⁴⁴ Lockheed Martin Advanced Technology Center, 3251 Hanover St., Palo Alto, CA 94304
- ⁴⁵ European Space Agency, European Space Operations Centre, Robert-Bosch-Strasse 5, 64293 Darmstadt, Germany
- ⁴⁶ TMT International Observatory, 100 W. Walnut Street, Suite 300, Pasadena, CA, 91124, USA
- ⁴⁷ ETH Zurich, Wolfgang-Pauli-Str 27, CH-8093 Zurich, Switzerland
- ⁴⁸ NASA Ames Research Center, Space Science and Astrobiology Division, MS 245-6, Moffett Field, CA, 94035, USA
- ⁴⁹ DTU Space, Technical University of Denmark. Building 328, Elektrovej, 2800 Kgs. Lyngby, Denmark
- ⁵⁰ Dept. of Astrophysics, University of Vienna, Türkenschanzstr 17, A-1180 Vienna, Austria
- ⁵¹ Deceased
- ⁵² Associated Universities for Research in Astronomy, Inc., 1331 Pennsylvania Avenue NW, Suite 1475, Washington, DC 20004, USA
- ⁵³ Institute for Astronomy, 640 N Aohoku Pl Hilo, HI 96720, USA
- ⁵⁴ UCO/Lick Observatory, University of California, Santa Cruz, CA 95064
- ⁵⁵ The University of Texas at Austin, Department of Astronomy RLM 16.342, Austin, TX 78712
- ⁵⁶ Department of Astronomy, Cornell University, Ithaca, NY 14853, USA
- ⁵⁷ Department of Physics and Astronomy, University of Victoria, Victoria, BC, V8P 5C2, Canada
- ⁵⁸ Dept. of Space, Earth and Environment, Chalmers University of Technology, Onsala Space Observatory, S-43992 Onsala, Sweden
- ⁵⁹ Johns Hopkins University Applied Physics Laboratory, 11100 Johns Hopkins Road, Laurel, MD 20723, USA
- ⁶⁰ Dept. of Physics & Astronomy, Johns Hopkins University, 3400 N. Charles St., Baltimore, MD, 21218, USA
- ⁶¹ Dublin Institute for Advanced Studies, School of Cosmic Physics, 31 Fitzwilliam Place, Dublin 2, D02 XF86, Ireland
- ⁶² Telespazio UK for the European Space Agency, ESAC, Camino Bajo del Castillo s/n, 28692 Villanueva de la Cañada, Spain
- ⁶³ Gemini Observatory/NSF's NOIRLab, 950 N. Cherry Avenue, Tucson, AZ, 85719, USA
- ⁶⁴ Blue Canyon Technologies, 5330 Airport Road, Boulder, CO, 80301, USA
- ⁶⁵ Aurora Technology for the European Space Agency, ESAC, Madrid, Spain
- ⁶⁶ HelioSpace Inc., 932 Parker St. Suite 2, Berkeley, CA, 94710, USA
- ⁶⁷ Cavendish Laboratory, University of Cambridge, 19 J. J. Thomson Ave., Cambridge CB3 0HE, UK
- ⁶⁸ Kavli Institute for Cosmology, University of Cambridge, Madingley Road, Cambridge CB3 0HA, UK
- ⁶⁹ Canadian Institute for Theoretical Astrophysics, University of Toronto, McLennan Physical Laboratories, 60 St. George Street, Toronto, Ontario, Canada M5S 3H8
- ⁷⁰ Astronomy Department, University of Michigan, Ann Arbor, MI 48109, USA
- ⁷¹ Quantum Circuits, Inc., New Haven, Connecticut, USA
- ⁷² Kapteyn Astronomical Institute, University of Groningen, P.O. Box 800, 9700 AV Groningen, The Netherlands
- ⁷³ Vantage Systems Inc, Greenbelt MD, 20706
- ⁷⁴ Howard Community College, Columbia MD, 21044
- ⁷⁵ Department of Astronomy, Oskar Klein Centre; Stockholm University; SE-106 91 Stockholm, Sweden
- ⁷⁶ Department of Physics and Astronomy, University of Rochester, Rochester NY 14627, USA
- ⁷⁷ Univ. Grenoble Alpes, CNRS, IPAG, F-38000 Grenoble, France.
- ⁷⁸ Katherine Johnson IV&V Facility, Goddard Space Flight Center, Code 180, Greenbelt, MD 20771
- ⁷⁹ Department of Physics & Astronomy, Bishop's University, Sherbrooke, QC J1M 1Z7, Canada.
- ⁸⁰ School of Physics & Astronomy, Space Research Centre, University of Leicester, Space Park Leicester, 92 Corporation Road, Leicester LE4 5SP, UK
- ⁸¹ Institute for Computational Astrophysics and Department of Astronomy & Physics, Saint Mary's University, 923 Robie Street, Halifax, NS B3H 3C3, Canada
- ⁸² Universities Space Research Association, 425 3rd Street SW, Suite 950, Washington DC 20024, USA
- ⁸³ Astrophysics Department, American Museum of Natural History, 79th Street at Central Park West, New York, NY 10024
- ⁸⁴ Department of History and Classics, University of Alberta, Edmonton, Alberta, Canada
- ⁸⁵ Princeton University, 4 Ivy Ln, Princeton, NJ 08544, USA

⁸⁶*National Optical-Infrared Research Laboratory, 950 N Cherry Ave, Tucson, AZ 85719*

⁸⁷*School of Earth and Space Exploration, Arizona State University, Tempe, AZ 85287-1404, USA*

⁸⁸*Universities Space Research Association, 425 3rd Street SW, Suite 950, Washington DC 20024, USA*

⁸⁹*AURA for the European Space Agency (ESA), ESA Office, Space Telescope Science Institute, 3700 San Martin Drive, Baltimore, MD 21218, USA*

ABSTRACT

Twenty-six years ago a small committee report, building on earlier studies, expounded a compelling and poetic vision for the future of astronomy, calling for an infrared-optimized space telescope with an aperture of at least $4m$. With the support of their governments in the US, Europe, and Canada, 20,000 people realized that vision as the $6.5m$ James Webb Space Telescope. A generation of astronomers will celebrate their accomplishments for the life of the mission, potentially as long as 20 years, and beyond. This report and the scientific discoveries that follow are extended thank-you notes to the 20,000 team members. The telescope is working perfectly, with much better image quality than expected. In this and accompanying papers, we give a brief history, describe the observatory, outline its objectives and current observing program, and discuss the inventions and people who made it possible. We cite detailed reports on the design and the measured performance on orbit.

1. INTRODUCTION

We summarize the history, concept, scientific program, and technical performance of the James Webb Space Telescope (JWST, Webb; Gardner et al. 2006). This paper points to and extracts key results from detailed papers in this issue on the four instruments: Near-Infrared Camera (NIRCam; Rieke et al. 2022, this issue), Near-Infrared Spectrograph (NIRSpec; Böker et al. 2023, this issue), Near-Infrared Imager and Slitless Spectrograph (NIRISS Doyon et al. 2023, this issue), and Mid-Infrared Instrument (MIRI; Wright et al. 2023, this issue); the telescope (McElwain et al. 2023, this issue); the observatory (Menzel et al. 2023, this issue); the scientific performance (Rigby et al. 2022a, this issue); and the brightness of the sky and stray light (Rigby et al. 2022b, this issue).

Launched 2021 December 25, the JWST (See figure 1) is a $6.5m$ diameter cold space telescope with cameras and spectrometers covering $0.6\mu m$ to $28\mu m$ wavelength. Orbiting the Sun-Earth L2 point, it extends the discoveries and technologies of the $2.4m$ warm Hubble Space Telescope (HST) and the $85cm$ cold Spitzer Space Telescope. JWST enables observations of the distant early universe, potentially reaching beyond redshift $z \sim 15$, within $\lesssim 300Myr$ of the Big Bang. JWST's infrared wavelength range penetrates dust clouds, to observe obscured active galactic nuclei (AGN) and star and planet formation. It shows objects too cool to radiate visible light. It includes the fundamental vibration-rotation bands of important molecules.

JWST was conceived from the beginning as an international project, led by NASA in partnership with the European and Canadian Space Agencies (ESA and CSA). Observing time allocations are open to all as-



Figure 1. JWST in the Northrop Grumman cleanroom following a sunshield deployment test.

tronomers worldwide. JWST was launched from French Guiana on an ESA-provided Ariane 5 rocket. JWST cost NASA \$8.8B to get to launch, and will make observations for a projected fuel-limited lifetime potentially as long as 20 yrs. JWST's observations cannot be obtained in any other way: Hubble has $1/6.25$ of the collecting area, and, being a room-temperature telescope emits its own infrared beyond $1.7\mu m$. Spitzer was cold but had less than 2% of JWST's collecting area. For ground-based telescopes, the Earth's warm atmosphere results in a background that is $10^6 - 10^7$ times higher and also blocks large regions of IR wavelengths.

JWST includes a general-purpose instrument package in its Integrated Science Instrument Module (ISIM). NIRCam covers $0.6\mu m$ to $5\mu m$ with filters, a corona-

graph, 0.032 arcsec pixels in its short wavelength channel, and a dichroic filter enabling simultaneous observation in both short and long wavelength bands. NIRSpec covers the same wavelength range with prisms and gratings, with fixed slits, an integral field unit (IFU), and a microshutter array (MSA) to select up to 100 simultaneous targets. NIRISS covers the same wavelength range with slitless spectroscopy, and provides a non-redundant mask for coronagraphy. MIRI covers $5\mu\text{m}$ to $28\mu\text{m}$ with imaging, IFU spectroscopy, and coronagraphs. The Fine Guidance Sensor (FGS) senses pointing errors and feeds the attitude control system to maintain sharp images. ESA provided the NIRSpec with the detectors and micro-shutter array provided by Goddard, CSA provided the NIRISS and FGS, and a partnership of JPL and a European consortium provided MIRI. NIRCam, and the US portions of MIRI and NIRSpec, were funded by NASA.

JWST’s first year of observations includes nearly half of a year of guaranteed time observations allocated to the teams building the instruments, 6 interdisciplinary scientists, and the telescope scientist. There is also a set of 13 competitively-selected Director’s Discretionary Early Release Science (DD-ERS) programs with data that become public immediately. The remaining observations were selected from over 1200 proposals through a dual-anonymous peer review, in which the identities of the proposers were not known to reviewers. Anyone can propose, regardless of nationality or institution. There were 286 programs selected in Cycle 1, including 263 pointed programs, 3 pure parallel programs, and 20 archival or theory programs. The Cycle 2 call received more than 1600 proposals submitted by more than 5000 scientists from around the world. NASA provides funding for data analysis to US-based investigators who are awarded time on JWST, and for archival and theoretical research related to JWST.

JWST is a technical pioneer, the first deployable segmented space telescope, with mirror segments that are aligned and focused after launch, with its remarkable cryogenic optical system providing diffraction-limited images (Strehl ratio 0.8) as short as $1.1\mu\text{m}$. Its detectors are larger and more sensitive than previous generations. Its 6.0K cryocooler for the mid IR instrument (MIRI) has no expendables and should last the duration of the mission. It uses cryogenic ASICs to control and read the near IR detectors. Its 5-layer sunshield cools the telescope to between 35K and 55K. Based on JWST’s successes and lessons learned, NASA is positioned to proceed to the 6m near-IR, optical, and UV flagship telescope recommended by the 2020 Decadal Survey (*National Academies of Sciences & Medicine 2021*), with

the ability to directly detect Earth-like planets around Sun-like stars.

2. TIMELINE HISTORY OF JWST

In this section we present a brief timeline history of the concept, design, construction and testing of JWST.

2.1. 1980s.

In the 1980s, preliminary work by Garth Illingworth, Pierre Bély, Peter Stockman, and others on an 8m to 10m passively-cooled infrared telescope began at Space Telescope Science Institute (STScI), following Riccardo Giacconi’s advice to work on the “next big thing.” Progress was reported at the STScI/NASA Next Generation Space Telescope (NGST) conference, 1989 September 13 to 15 (*Bely et al. 1990*). This international conference excited scientists and engineers with the scientific opportunities and technical challenges enabled by a very large cold infrared space telescope. A decade before that, in 1979, a National Academy of Sciences (NAS) report recommended the Shuttle Infrared Telescope Facility (SIRTF, later Spitzer; *Field & Astronomy and Astrophysics Survey Committee 1983*), even before the IRAS launch (1983 January 25). Goddard built the Cosmic Background Explorer (COBE) and launched it on 1989 November 18 to measure the Big Bang, the cosmic microwave and IR background light, beginning the era of precision cosmology (*Mather et al. 1994*). The discovery of the primeval anisotropy led to the standard model of cosmology, in which gravity acting on density fluctuations could produce galaxies. To build the COBE, Goddard also developed expertise with cryogenic instrumentation and test programs that would become essential for Webb.

2.2. 1990s.

The Hubble was launched 1990 April 24 and its optical error was soon discovered, leading to two breakthroughs: learning to measure the optical error (spherical aberration) with phase diversity, and demonstrating the value of the planned servicing and repair of Hubble using the Space Shuttle in 1993. The development of the phase diversity algorithms was jointly done by STScI, Goddard and JPL (*Burrows et al. 1991; Fienup et al. 1993; Krist & Burrows 1995*). The experience gained by the people working on the servicing missions, instrument upgrades, and spacecraft hardware repairs and replacements would be critically important for the development of the JWST, as many of the younger engineers working on Hubble later became leaders of the Webb team. The Bahcall report (Decadal Survey: *Bahcall & Astronomy and Astrophysics Survey Committee*

1991) endorsed Spitzer (at that time called the Space Infrared Telescope Facility, SIRTf) and declared that the 1990s would be the “Decade of the Infrared.” The AstroTech conference (Illingworth 1991) reviewed possibilities for large telescopes and cited the Bahcall report. In 1993, the Edison mission, a deployable 2m+ diameter IR telescope, was proposed to ESA (Thronson et al. 1996). Larger format IR detector arrays, in part spurred by the NICMOS development, enabled galaxy surveys (e.g., Gardner et al. 1993) and other near-IR science with ground-based telescopes.

The Edison concept included passive cooling, and some of the people working on Edison brought that experience to the JWST team later. The Hubble phase retrieval algorithm was published and the Hubble optics were corrected in its first servicing mission. Soon after, NASA commissioned AURA’s HST and Beyond committee, chaired by Alan Dressler, to write a report on potential successors to HST (Dressler & HST and Beyond Committee 1996). STScI sent a proposal entitled “High-Z” to NASA, suggesting that a telescope in a 1×3 AU long elliptical orbit would be helpful, to get outside the interference of the zodiacal dust cloud. In 1995, JPL submitted the MIRORS proposal to NASA for a passively cooled mid IR telescope (Wade et al. 1996).

2.2.1. 1995.

On 1995 October 30, Ed Weiler of NASA HQ left a phone message for John Mather at Goddard, explaining that NASA was starting a study of what was then called the Next Generation Space Telescope (NGST), and inviting his participation. Within the context of the previous studies, and based on a draft of the HST and Beyond report, NGST would be a 4m passively-cooled IR telescope making observations at $1\mu m < \lambda < 5\mu m$. GSFC chose Bernie Seery to manage the study. The Federal Government shut down 1995 November 14 to 19 and again 1995 December 16 to 1996 January 6. On 1996 January 6 to 8, a record blizzard closed the Washington DC area and nothing moved for a week. As a result Mather did not attend the dramatic AAS meeting in San Antonio. This pivotal start foreshadowed Webb’s future, as its development was to be affected by more storms, government shutdowns, a terrorist attack, an earthquake in Virginia, a lightning strike, a hurricane in Texas, and the COVID pandemic, all of which would occur before Webb was launched.

On 1996 January 15, the Hubble Deep Field image was released at the AAS meeting, completely changing our view of galaxies in the universe (Williams et al. 1996). On 1996 January 17, Dan Goldin spoke to the AAS, saying, “Why do you ask for such a modest

thing [4m]? Why not go after six or seven meters?” He received a standing ovation, which turned out to be Webb’s first (informal) peer review. Dressler also spoke to present the report at the meeting (Dressler & HST and Beyond Committee 1996). On 1996 January 22 to 25, Mather attended a conference in Johannesburg, and met ESA counterparts for the first time to discuss ideas for the NGST. The final Dressler report appeared in 1996 May (Dressler & HST and Beyond Committee 1996). Wendy Freedman’s Hubble Key Project reported on the Hubble Constant, discussing their initial values (around $60 km s^{-1} Mpc^{-1}$) and comparing to others (up to $80 km s^{-1} Mpc^{-1}$) (Freedman et al. 2001, and references therein). Predictions of early galaxies that could be visible to Webb depend strongly on this number, and would be important when a descope decision was taken in 2001.

2.2.2. 1996 to 1999.

The year 1996 marked the industrial kickoff. Around May, GSFC presented NGST ideas to interested aerospace companies in a meeting held at the Space Telescope Science Institute (STScI). NASA issued a Cooperative Agreement Notice so the companies could compete for this new work. Two studies were chosen (TRW and Ball) and they and the Government/STScI teams reported in September. Jonathan Gardner, newly hired at Goddard, attended the meeting, learning about NGST for the first time. The reports said they could meet Goldin’s cost target of \$0.5B, though what exactly was included in these estimates is unclear now. Outside this group, hardly anyone believed that such a low cost was possible.

In 1997, NASA solicited proposals for the Ad Hoc Science Working Group to advise NASA on the choice of scientific objectives and instruments; the committee first met later that year. In 1997, AURA issued a report “Visiting a Time When Galaxies were Young”, detailing the concepts that had been developed in 1996 (Stockman 1997). In 1998, a conference in Liège, Belgium reported progress developing science drivers and technological challenges (Kaldeich-Schürmann 1998), after ESA established an NGST Task Force. The STScI was officially made the NGST Science Operations Center in a ceremony with Senator Barbara Mikulski and Administrator Goldin. The cosmic acceleration (dark energy) was discovered (Riess et al. 1998; Schmidt et al. 1998; Perlmutter et al. 1999), adding to the growing sense that NGST was key to studies of the distant universe, as a dark-energy-dominated universe has galaxies forming at higher redshift than in a matter-dominated flat universe. The conference “Science with the NGST (Next Gener-

ation Space Telescope)” was held at GSFC (Smith & Koratkar 1998).

On July 7, NASA selected Lockheed Martin and TRW to conduct Phase A mission studies, preliminary analysis of the design, and cost. Discussions began with international partners about their possible roles as ESA, CSA and the Japanese Space Agency (JAXA) participated in the ASWG. In September, just as hurricane Floyd approached, the NGST Science and Technology Exposition was held in Hyannis, MA and the choices of possible near IR spectrometer designs were presented (Smith & Long 2000). Mather & Stockman (2000) reported the early history of NGST and listed the instrument studies then underway. The MEMS (microelectromechanical system) concept for a multi-object spectrometer was favored over a Fourier spectrometer, because the Fourier multiplex advantage does not apply if most of the sky is empty and detector noise is not high (Gardner & Satyapal 2000). Moseley et al. (1999) described the microshutter array, which has significant advantages in size, contrast and cryogenic operation over the micromirror arrays developed by Texas Instruments for digital light projection (MacKenty & Stiavelli 2000).

The ASWG final report recommended that NGST include a NIRCam, NIRSpec with a MEMS-based multi-object spectrograph capability and a MIRI doing both imaging and spectroscopy. They gave three options for a fourth instrument: a tunable filter, a visible-light camera and an integral-field spectrograph (Stockman & Mather 2001). By this time, JAXA had decided not to participate in the mission, and the ASWG recommended that NASA partner with ESA and CSA.

2.3. 2000s

Ed Weiler signed the Formulation Authorization Document in 1999, defining NGST as a NASA priority, but a mid-infrared instrument was a goal rather than a requirement. The 2000 Decadal Survey ranked NGST #1 in large space missions (McKee et al. 2001). The ranking was predicated on the inclusion of a mid-infrared instrument, which established it as a requirement for the mission. NASA chose an Interim Science Working Group (ISWG) to write the specifications for the instruments and advise about the telescope. NASA and ESA formed a joint Mid-Infrared Steering Committee, which developed a concept for a mid-infrared instrument (MIRI) doing both imaging and spectroscopy. The agencies negotiated a partnership in which ESA would provide the optical bench and NASA would provide the detectors and cooling system.

In 2001, while preparing the statement of work for the solicitation of the main industrial contract, Goddard

descope the telescope from $50m^2$ to $25m^2$ in collecting area, or $8m$ to $6.5m$ diameter. The descope was to address a mismatch between the budget and the scope in the solicitation. In mid-2002, NASA chose TRW to build the observatory, reserving the ISIM to be built by Goddard. NASA renamed NGST for James E. Webb, who was the second administrator of NASA, from 1961 to 1968. Webb was responsible for getting astronauts to the Moon in 8 years, and for expanding NASA’s science program, which built space telescopes, sent probes to Venus and Mars, and started missions to the outer planets (Lambright 1995).

In 2002, NASA selected a proposal led by Marcia Rieke of the University of Arizona to build the NIR-Cam. In the same proposal call, NASA selected several members of the flight Science Working Group (SWG; see Table 1), including 6 interdisciplinary scientists and the US members of the MIRI science team. NASA signed MOUs with ESA and CSA detailing the international partnership. ESA would provide the launch vehicle, the NIRSpec and the optical bench for MIRI. CSA would provide the FGS, and install a tunable-filter imager (TFI) on the other side of the FGS optical bench. The development of a cryogenic etalon meeting the requirements for the TFI would prove to be challenging and ultimately was not successful. The SWG also includes NASA Project Scientists and representatives of the partner agencies.

Phil Sabelhaus was selected as the Project Manager as the project entered its detailed design phase. In late 2003, the part of TRW selected to build JWST was acquired by Northrop Grumman. Northrop, in consultation with Goddard and the optics Product Integrity Team, selected beryllium for the mirror material. The competing glass sandwich technology had failed to meet its figure stability requirements (Stahl et al. 2004). In addition, the Spitzer Space Telescope (building on other IR space missions) had demonstrated that construction of a high-precision beryllium mirror was possible. In 2003, the fabrication of the flight mirrors began by Northrop through a sub-contract to Ball Aerospace.

Beginning the mirrors was a key step and reflected the expectation that they could be a critical path pacing item. The Spitzer Space Telescope was launched 2003 August 25. Spitzer rapidly demonstrated the power of mid-IR space missions (e.g., Werner et al. 2004), and confirmed the wisdom of including the MIRI in JWST. On 2004 March 3, construction officially began for the JWST. In 2005, in order to conserve mass, a helium pulse tube cryocooler to be built by Northrop Grum-

Table 1. The JWST Science Working Group

| Name | Institution | Position |
|--------------------|--------------------------|--|
| Santiago Arribas | CSIC | NIRSpec Science Representative * |
| Mark Clampin | NASA/HQ | Observatory Project Scientist * |
| René Doyon | Univ of Montreal | CSA Representative |
| Pierre Ferruit | ESA | ESA Representative |
| Kathryn Flanagan | STScI, retired | STScI Representative * |
| Marijn Franx | Leiden University | NIRSpec Science Representative * |
| Jonathan Gardner | NASA/GSFC | Deputy Senior Project Scientist |
| Matthew Greenhouse | NASA/GSFC | ISIM Project Scientist |
| Heidi Hammel | AURA | Interdisciplinary Scientist |
| John Hutchings | DAO, retired | CSA Representative * |
| Peter Jakobsen | ESA, retired | ESA Representative * |
| Jason Kalirai | JHU/APL | STScI Representative * |
| Randy Kimble | NASA/GSFC | Integration, Test, & Commissioning Project Scientist |
| Nikole Lewis | Cornell University | STScI Representative * |
| Simon Lilly | ETH Zurich | Interdisciplinary Scientist |
| Jonathan Lunine | Cornell University | Interdisciplinary Scientist |
| Roberto Maiolino | University of Cambridge | NIRSpec Science Representative |
| John Mather | NASA/GSFC | Senior Project Scientist |
| Mark McCaughrean | ESA | Interdisciplinary Scientist |
| Michael McElwain | NASA/GSFC | Observatory Project Scientist |
| Matt Mountain | AURA | Telescope Scientist |
| Malcolm Niedner | NASA, retired | Deputy Senior Project Scientist/Technical |
| George Rieke | University of Arizona | MIRI Science Lead |
| Marcia Rieke | University of Arizona | NIRCam Principal Investigator |
| Jane Rigby | NASA/GSFC | Operations Project Scientist |
| Hans-Walter Rix | Max Planck Institute | NIRSpec Science Representative * |
| George Sonneborn | NASA, retired | Operations Project Scientist * |
| Massimo Stiavelli | STScI | Interdisciplinary Scientist |
| H. Peter Stockman | STScI, retired | STScI Representative * |
| Jeff Valenti | STScI | STScI Representative |
| Chris Willott | CNRC | NIRISS Science Lead |
| Rogier Windhorst | Arizona State University | Interdisciplinary Scientist |
| Gillian Wright | UKATC | MIRI European Principal Investigator |

NOTE—The JWST Science Working Group (SWG) consists of GTOs, NASA Project Scientists, and representatives from ESA, CSA and STScI. (*) designates a former member who was replaced by someone else. The NIRSpec Science Representative position rotated through several members of the NIRSpec team. The SWG first met on 2002 August 19 and disbanded at the end of JWST Commissioning, 2022 July 12.

man was chosen to replace the planned solid hydrogen cooler for the MIRI. Gardner et al. (2006) published a special issue of the journal *Space Science Reviews*, detailing the JWST science objectives and design. In 2005 Mike Griffin replaced Sean O’Keefe as NASA Administrator, and in 2007, Griffin approved the contribution of the European Ariane 5 rocket for JWST. The final servicing mission for HST was conducted in 2009, freeing

the large cleanroom at Goddard for the integration of the JWST instruments into the ISIM, the integration of the Optical Telescope Element (OTE), and the assembly of the ISIM and the OTE.

2.4. 2010s.

In 2010, CSA realized that they would not be able to deliver the tunable filter imager on schedule, re-

moved the etalon, and redesigned the camera as the NIRISS (Doyon et al. 2012). The near-infrared detectors were found to be degrading, and it became clear that they would have to be replaced (Rauscher et al. 2014; Rauscher 2014). The spacecraft and sunshield were also behind schedule.

Budget troubles mounted, and Senator Mikulski asked for an independent review and a realistic budget estimate that would not grow every year. Congress was very skeptical of the planned 2014 launch date and the budget. The HgCdTe detectors were found to be degrading in storage, and a new version was ordered. NASA responded to the growing concerns around schedule and cost, by setting up a Test Assessment Team for advice on the testing path forward. In response to Senator Mikulski’s request for a full review of what was going wrong, the NASA Administrator set up the Independent Comprehensive Review Panel (ICRP). The ICRP report was hard hitting and direct, confirming the basic soundness of the mission and concurring with the recommendations of Project management that additional budget and schedule were needed. The formal recommendations were all accepted by the Administrator. The ICRP emphasized the scientific value of JWST, but outlined the budgetary issues that had plagued the Project and recommended that a thorough Joint Cost and Schedule assessment be done quickly. Project Manager Phil Sabelhaus was replaced by Bill Ochs. In 2011, that budget assessment was finished, and indicated that it would take a total budget of \$8B to complete JWST with a launch in 2018, 4 years later than planned.

Frustration with JWST led to a proposed zero budget by the House Appropriation Sub-Committee on 2011 July 7. A grassroots public effort was undertaken to support Senator Mikulski’s efforts to restore the budget. The public support was remarkable. The effort paid off and agreement was reached to restore JWST. JWST’s budget of \$8.0B to launch was approved by Congress late in 2011, but with strong language capping the cost. In 2012, the MIRI and NIRISS/FGS instruments arrived at GSFC. A Derecho storm cut off all three electrical power lines to GSFC in the middle of a cryo-vacuum test, but there was no damage to the JWST hardware. In 2013 the NIRCams and NIRSpec arrived at GSFC, and the four instruments were assembled into the ISIM by 2014. Altogether three cryo-vac tests were done on the instrument module (Kimble et al. 2016; Greenhouse 2019), and it was assembled to the telescope and given vibration and acoustic tests at GSFC. Challenges during the three cryo-vac tests included a major snowstorm, a lightning strike on the building and a fire in the clean room prompting evacuation of the personnel. No people

or flight hardware were harmed in these events, which took place between 2014 and 2016.

The eighteen primary mirror segments, the secondary mirror, the tertiary mirror, and the fine-steering mirror are all made of beryllium with a gold optical coating. Of the 18 primary mirror segments, there are 6 each of 3 optical prescriptions, to enable the six-fold symmetry of the primary mirror. Three spare mirrors, one of each optical prescription, were also prepared. In order to meet the $25nm$ root-mean-squared surface figure requirement for each mirror segment, the mirrors were initially polished to a surface accuracy of about $100nm$, using an iterative process. The segments’ surface figures were then measured at the cryogenic operating temperature in the X-Ray and Cryogenic Facility (XRCF) at NASA’s Marshall Space Flight Center. Using those cryogenic measurements, the segments were polished again so that they would meet the surface figure at their operating temperature. The secondary, tertiary and FSM were treated in a similar manner. The mirrors were then coated, underwent environmental testing, and acceptance testing at the operating temperatures was conducted again in the XRCF. The individual mirrors were complete by early 2012 (Feinberg et al. 2012).

With the mirrors complete, the hexapod actuators were assembled onto each mirror. Assembly of the primary mirror segments onto the backplane took place at Goddard during late 2015 and early 2016. The integration of the ISIM onto the back of the primary mirror was complete by 2016 May 24, at which time, the assembled Optical Telescope element and ISIM became known as OTIS. Vibration and acoustic testing took place over the following year.

On 2017 May 7 the OTIS was flown to NASA’s Johnson Space Center on a C5C aircraft, and spent 6 months there, including a 100-day full scale cryo-vac test (see Figure 2), right through Hurricane Harvey and 1.3m of rain (Kimble et al. 2018). On 2018 February 2 the OTIS arrived at Northrop Grumman in Redondo Beach for integration with the warm spacecraft and sunshield, which themselves were undergoing their element-level acoustic and vibration tests (Menzel et al. 2023, this issue). In 2017, delays in the spacecraft (e.g., propulsion system welding problems) and the sunshield development at Northrop began to indicate that a 2018 launch was not likely. By early 2018 it was clear that added time and money was needed, and another Independent Review Team was set up. They emphasized “mission success” but noted that a launch delay was inevitable for the integration and testing (I&T) that remained. In 2018 May, loose screws and washers were found after a vibration test of the sunshield, making it clear that

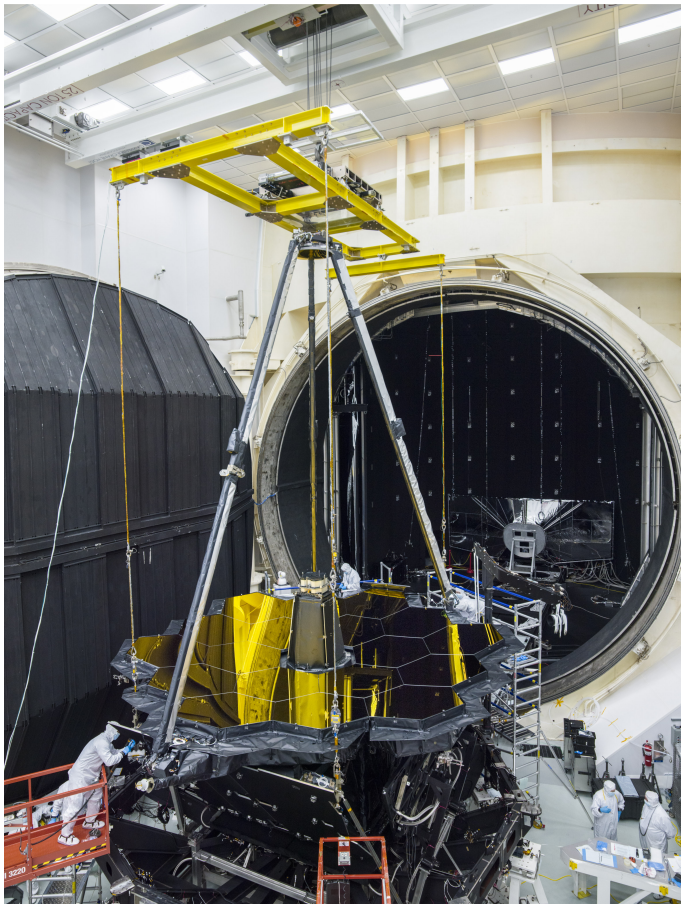


Figure 2. The JWST telescope and ISIM in preparation for the OTIS thermal vacuum test at the Johnson Space Center's historic Chamber A.

a significant delay was necessary to get JWST back on track. Rework of the sunshield followed. A new launch date in 2020 was selected as likely.

During this decade the Mission Operations Center was being set up at STScI, and a major software development effort was being undertaken by STScI with GSFC management for mission operations, science support and science operations. The JWST Science Advisory Committee (JSTAC) was chartered to help STScI and NASA develop science policies and approaches with the explicit goal of “maximizing the scientific return” from JWST. The JSTAC met for 8 years in parallel to the SWG. Both advisory committees were eventually succeeded by the JWST Users Committee (JSTUC).

2.5. 2020s.

Progress was good but the complexities of the I&T activities led to a further delay into 2021, compounded by the global coronavirus pandemic. In 2020 March, COVID-19 forced nationwide closures and NASA telework, but aerospace workers at the Northrop Grumman

facility in California were permitted to work under enhanced COVID-19 safety procedures. After the final vibration and acoustic test in 2020, the flight transponders failed in early 2021 and were returned to the manufacturer for repair. Flight rehearsals began in the Mission Operations Center in 2020, using the digital twin, an observatory simulator that is still in use today for verification of command sequences. Some of the rehearsals included remote or hybrid participation due to the pandemic; this would prove valuable experience during commissioning.

The final I&T work in 2021 went extremely well, adding to confidence that the spacecraft and sunshield were becoming mature and ready for launch. On 2021 October 21, JWST arrived at the launch site in French Guiana on the MN Colibri ship, after passing through the Panama Canal. On 2021 December 25 at 12:20 UTC, the Ariane 5 launched the Webb exactly as planned, with a flawless launch and positioning of JWST for its trajectory to L2 (see figure 3). The launch went so well that the propellant needed to adjust its trajectory to L2 and the insertion were much less than budgeted. The propellant available for orbit adjustment will likely allow a mission life extension to a predicted 20 years, far larger than the 10-year goal.

2.5.1. 2022.

The first two weeks of “deployment terror” went remarkably well, with almost no unexpected issues. In particular, the sunshield with its 140 release mechanisms deployed successfully. The years of careful testing and checking had paid off. The following two weeks of mirror deployments also went smoothly and JWST was inserted into its L2 orbit 29 days after launch, ready for the slow, crucial process of aligning the mirrors. The outcome was that the optical performance and stability exceeded the requirements, with $1.1\mu\text{m}$ diffraction-limited imaging at NIRC*am*, almost twice as good as the requirement ($2\mu\text{m}$) (McElwain et al. 2023, this issue).

Despite the spike in COVID-19 cases at the end of 2021, the careful protocols developed and rehearsed by the Mission Operations Team enabled staffing of all critical ground-support positions throughout launch and early commissioning. Precautions included an expansion of the space used by the Mission Operations Center (MOC) at STScI, to permit socially-distanced staffing; greater reliance on remote support; mandated vaccination or testing, mandated masking, and electronic contact tracing for personnel in the MOC; and rapid antigen testing every other day for on-site staff.

Overall, commissioning the observatory went extremely smoothly in the MOC, due to the prior tests

and rehearsals, and especially the competence, focus and leadership throughout the NASA, Northrop, Ball, STScI, instrument teams, and other contractor teams. Everything on JWST works! Commissioning was completed and all 17 instrument modes were approved for scientific use by 2022 July 10. During commissioning, 120 hours were devoted to Early Release Observations (ERO Pontoppidan et al. 2022). The ERO of SMACS 0723 was announced by President Biden at the White House July 11 (Figure 4), and Stephan’s Quintet, the Carina Nebula, the Southern Ring Nebula, and WASP-96b were released on July 12. The data were released through the archives at the Mikulski Archive for Space Telescopes (MAST) on 2022 July 14; the release also included the commissioning data and online documentation of the scientific performance.

3. SCIENCE SCOPE

JWST was designed to address four science themes (Gardner et al. 2006), which trace cosmic history from the Big Bang to planets conducive to life. The End of the Dark Ages: First Light and Reionization theme seeks to identify the first luminous sources to form and to determine the ionization history of the early universe. The Assembly of Galaxies theme seeks to determine how galaxies and the dark matter, gas, stars, metals, morphological structures, and active nuclei within them evolved from the epoch of reionization to the present day. The Birth of Stars and Protoplanetary Systems theme seeks to unravel the birth and early evolution of stars, from infall on to dust-enshrouded protostars to the genesis of planetary systems. The Planetary Systems and the Origins of Life theme seeks to determine the physical and chemical properties of planetary systems including our own, and investigate the potential for the origins of life in those systems.

Observing time on JWST has been allocated by three methods: Guaranteed Time Observations (GTO), General Observers (GO) time, and Director’s Discretionary (DD) time. The GTO time consists of 4020 hours of JWST observations over the first three years, allocated to the four instrument teams and other scientists on the Science Working Group. The DD time consists of 10% of the time available for the lifetime of the mission. The GO time is the remainder.

The GTO allocations are listed in Table 2. Changes from the original allocations are due to programs shared between the GTOs and to changes in the overheads that occurred after the selected observations were specified prior to the Cycle 1 Call For Proposals. The GTO scientists chose to allocate the majority of the GTO time in Cycle 1, leaving just 196.1 hours of observation time

for Cycles 2 and 3. The table shows the amount of time executed as of 2022 September 30. Further updates are available from <https://www.stsci.edu/cgi-bin/get-jwst-gto-time>.

The DD time is allocated by the Director of JWST’s Science and Operations Center (SOC), located at the Space Telescope Science Institute. In 2018, following a recommendation by the JSTAC, Director Ken Sembach allocated up to 525 hours of Cycle 1 DD time to the DD-Early Release Science Program (Levenson & Sembach 2018). The DD-ERS program was designed and implemented by Janice Lee, Jennifer Lotz and Neill Reid. It consists of 13 peer-review selected programs designed to demonstrate JWST’s capabilities and provide open-access data to the community early in the mission. The DD-ERS programs were intended to be conducted within the first 3 to 5 months of Cycle 1; Table 3 lists the programs.

Observing time on JWST is allocated by wall-clock time; all overheads are included in the time allocated. Overheads that are determined by the observing sequence, such as slews or mechanism movements, are accounted by the planning software. Overheads that are independent of the specific observations, such as the calibration program or station-keeping maneuvers, are accounted by a percentage of time applied to each program.

The Cycle 1 GO program allocated approximately 6000 hours. Between the GTO, DD and GO programs, the total number of hours in Cycle 1 exceeds 1 year (8760 hours) by about 25%. The field of regard of JWST is about 40% of the sky at any given time. There will need to be enough targets within the field of regard at the end of Cycle 1 to efficiently schedule the observations, and the extra 25% tail will ensure a smooth transition from the end of Cycle 1 to the beginning of Cycle 2. The remaining allocated Cycle 1 observations will be conducted during the early months of Cycle 2, and there will be a similar transition from Cycle 2 to Cycle 3.

3.1. Director’s Discretionary Early Release Observation programs

The DD-ERS program consists of 13 programs ranging from the early Universe to our Solar System. Collectively the programs use most of the JWST instrument modes; the data taken have no exclusive access period so that prior to writing Cycle 2 observing proposals, the scientific community were able to obtain JWST data

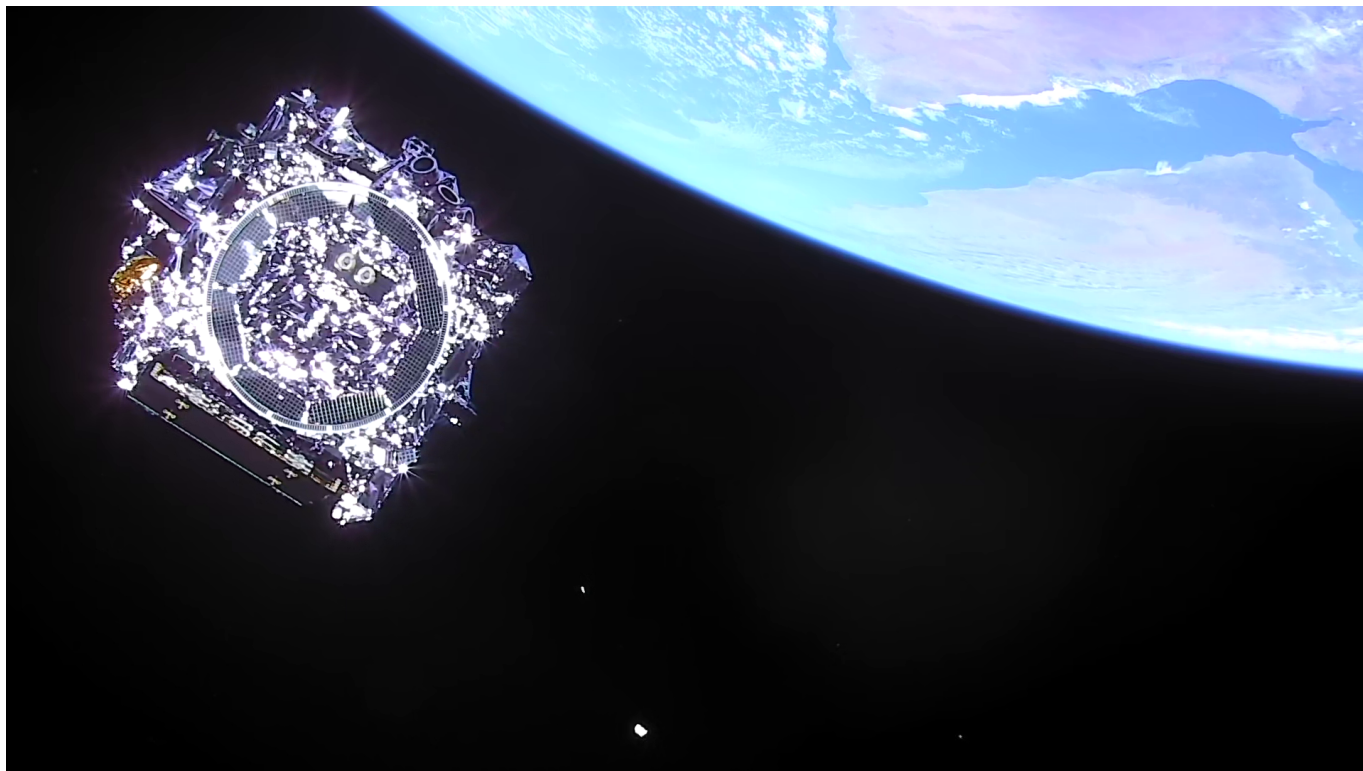


Figure 3. JWST viewed from a camera in the upper stage of the Ariane 5 launch vehicle, just after separation. The Gulf of Aden and the east coast of Africa are visible in the upper right. This still from a video is courtesy ESA and Arianespace. The full video is available at: https://www.esa.int/ESA_Multimedia/Videos/2021/12/Webb_separation_from_Ariane_5.



Figure 4. JWST's first released image, the lensing cluster SMACS 0723, was the deepest infrared image ever taken.

from the archive that is relevant to their proposals. In this section we describe the DD-ERS programs, and report on those that had early scientific results that were published or submitted by 2022 September 30.

3.1.1. *DD-ERS 1288; PDRs4All: Radiative Feedback from Massive Stars*

Massive stars produce intense winds and radiation which ionizes and heats the surrounding molecular cloud material, affecting future star formation in the cloud. These interactions create Photo-Dissociation Regions (PDRs), which dominate the infrared spectra of star-forming galaxies and drive the evolution of star formation from interstellar matter. PDRs4All (Berné et al. 2022) consists of NIRCам and MIRI imaging and MIRI MRS and NIRSpec IFU spectroscopy of PDRs in the Orion Bar.

3.1.2. *DD-ERS 1309; IceAge: Chemical Evolution of Ices During Star Formation*

Icy grain mantles hold volatile elements and prebiotic complex organic molecules in star-forming regions. IceAge (McClure et al. 2018; McClure 2022) will use NIRSpec and MIRI spectroscopy and NIRCам wide-field slitless spectroscopy to study ice chemistry in a representative low-mass star-forming region at sev-

Table 2. GTO Allocations

| Team | PI | Original | Current | Remaining | Executed |
|---------------------|------------------------|----------|---------|-----------|----------|
| MIRI STScI | Christine Chen | 12.0 | 10.5 | 1.5 | 0.0 |
| NIRISS Team | Rene Doyon | 450.0 | 469.2 | 6.9 | 34.9 |
| NIRSpec Team | Pierre Ferruit | 900.0 | 829.8 | 59.4 | 57.2 |
| MIRI STScI | Scott Friedman | 12.0 | 15.5 | 0.9 | 0.0 |
| MIRI STScI | Karl Gordon | 12.0 | 0.0 | 0.0 | 0.0 |
| MIRI US | Thomas Greene | 60.0 | 75.0 | 0.2 | 15.8 |
| IDS | Heidi Hammel | 110.0 | 141.5 | 1.0 | 32.7 |
| MIRI STScI | Dean Hines | 12.0 | 15.8 | 0.1 | 1.3 |
| IDS | Simon Lilly | 110.0 | 115.9 | 0.1 | 18.6 |
| IDS | Jonathan Lunine | 110.0 | 110.5 | 2.0 | 39.4 |
| IDS | Mark McCaughrean | 110.0 | 100.4 | 33.3 | 12.0 |
| MIRI US | Margaret Meixner | 60.0 | 76.2 | 0.3 | 26.6 |
| Telescope Scientist | Matt Mountain | 210.0 | 212.9 | 10.4 | 9.5 |
| MIRI STScI | Alberto Noriega-Crespo | 12.0 | 10.7 | 0.1 | 0.0 |
| MIRI US | Michael Ressler | 60.0 | 63.5 | 0.7 | 2.4 |
| MIRI Science Lead | George Rieke | 210.0 | 183.1 | 39.2 | 0.0 |
| NIRCam Team | Marcia Rieke | 900.0 | 1041.2 | -3.9 | 108.3 |
| IDS | Massimo Stiavelli | 110.0 | 110.0 | 25.7 | 5.1 |
| IDS | Rogier Windhorst | 110.0 | 122.0 | 0.2 | 23.4 |
| MIRI Europe | Gillian Wright | 450.0 | 452.0 | 18.0 | 62.9 |
| Totals | | 4020.0 | 4155.7 | 196.1 | 449.8 |

NOTE—The time allocations to GTO teams in hours. IDS stands for Interdisciplinary Scientist on the Science Working Group. The original allocations to each team (as set by policy and international agreements) have been modified due to exchanges or collaborations between GTO teams, and due to changes in overhead calculations since the original programs were submitted. The column labeled “Remaining” refers to the number of hours remaining to be allocated in Cycle 2 or Cycle 3. The number of hours in the final column are those that have been executed by 2022 September 30. The current values of the information listed in this table are available from <https://www.stsci.edu/cgi-bin/get-jwst-gto-time>

eral stages: pre-stellar core, Class 0 protostar, Class I protostar and protoplanetary disk. The program will map the spatial distribution of ices to 20 to 50 AU. If the organic molecules survive protostellar infall intact, then the molecular cloud could provide the precursors of biomolecules to the planetary systems that form within it, which could mean that life is a common outcome of star and planetary system formation.

3.1.3. *DD-ERS 1324; Through the looking GLASS: a JWST exploration of galaxy formation and evolution from cosmic dawn to present day*

Gravitational lensing by a Frontier Field cluster allows JWST to reach intrinsically faint galaxies in the epoch of reionization. GLASS (Treu et al. 2022b) will observe Abell 2744 with NIRSpec multi-object spectroscopy and NIRISS wide-field slitless spectroscopy, and will also cre-

ate a parallel deep field with NIRCam imaging. The parallel field will contain the deepest extragalactic data of the DD-ERS program; the spectroscopy will also be the deepest DD-ERS data obtained in those modes.

GLASS will identify galaxies within the epoch of reionization and measure Ly α velocities and morphologies, rest-frame UV and optical emission line fluxes and UV/optical photometry and sizes. The program will map metallicity, dust and star-formation rate for galaxies spanning $\log M_{\star} \sim 6$ to 10 at $z > 2$, when disks and bulges emerged and feedback was most active. The GLASS NIRISS observations will map systems at $z < 3.5$ and $\log M_{\star} \gtrsim 6$. The higher resolution NIRSpec observations will spectrally resolve key diagnostic lines which are blended at the lower resolution of the grism spectra. NIRSpec will also reach beyond $z \gtrsim 4$ galaxies.

Table 3. DD-ERS Programs

| ID | Acronym | Title | PI and Co-PIs | Instruments |
|------|------------|---|--|---------------|
| 1288 | PDRs4All | Radiative Feedback from Massive Stars as Traced by Multiband Imaging and Spectroscopic Mosaics | Olivier Berne, Emilie Habart, Els Peeters | M, NC, NS |
| 1309 | IceAge | IceAge: Chemical Evolution of Ices during Star Formation | Melissa McClure, Abraham C. Boogert, Harold Linnartz | M, NC, NS |
| 1324 | GLASS | Through the Looking GLASS: A JWST Exploration of Galaxy Formation and Evolution from Cosmic Dawn to Present Day | Tommaso Treu | NC, NI, NS |
| 1328 | GOALS-JWST | A JWST Study of the Starburst-AGN Connection in Merging LIRGs | Lee Armus, Aaron Evans | M, NC, NS |
| 1334 | | The Resolved Stellar Populations Early Release Science Program | Daniel Weisz | NC, NI |
| 1335 | Q-3D | Q-3D: Imaging Spectroscopy of Quasar Hosts with JWST Analyzed with a Powerful New PSF Decomposition and Spectral Analysis Package | Dominika Wylezalek, Sylvain Veilleux, Nadia Zakamska | M, NS |
| 1345 | CEERS | The Cosmic Evolution Early Release Science (CEERS) Survey | Steven Finkelstein | M, NC, NS |
| 1349 | WR DustERS | Establishing Extreme Dynamic Range with JWST: Decoding Smoke Signals in the Glare of a Wolf-Rayet Binary | Ryan Lau | M, NI |
| 1355 | TEMPLATES | TEMPLATES: Targeting Extremely Magnified Panchromatic Lensed Arcs and Their Extended Star Formation | Jane Rigby, Joaquin Vieira | M, NC, NS |
| 1364 | | Nuclear Dynamics of a Nearby Seyfert with NIRSpec Integral Field Spectroscopy | Misty Bentz | NS |
| 1366 | | The Transiting Exoplanet Community Early Release Science Program | Natalie Batalha, Jacob Bean, Kevin Stevenson | M, NC, NI, NS |
| 1373 | | ERS Observations of the Jovian System as a Demonstration of JWST’s Capabilities for Solar System Science | Imke de Pater, Thierry Fouchet | M, NC, NI, NS |
| 1386 | | High Contrast Imaging of Exoplanets and Exoplanetary Systems with JWST | Sasha Hinkley, Andrew Skemer, Beth Biller | M, NC, NI, NS |

NOTE—The 13 selected Director’s Discretionary – Early Release Science Programs. Instruments: NC = NIRCcam, NI = NIRISS, NS = NIRSpec, M = MIRI.

The NIRCcam parallel observations will cover $\sim 18\text{arcmin}^2$ in two regions. They will use 7 broadband filters from F090W to F444W, and will reach 5σ limits of 29.2 to 29.7 AB magnitudes (according to the pre-launch exposure time calculator.)

The GLASS team has published a series of papers with initial results, and other groups have also used these public data. The GLASS team papers include: (1) lensed galaxies at $z > 7$ (Roberts-Borsani et al. 2022), (2) photometry and catalogs (Merlin et al. 2022), (3) galaxies at $z > 9$ (Castellano et al. 2022), (4) metallicity in low-mass galaxies at $z \sim 3$ (Wang et al. 2022), (5) the size-luminosity relation at $z > 7$ (Yang et al. 2022), (6) measurements of rest-frame optical lines (Boyett et al. 2022), (7) globular clusters at $z \sim 4$ (Vanzella et al. 2022), (8) the detection of a lensed star at $z = 2.65$ (Chen et al. 2022b), (9) spectra of low-mass galaxies

at $z \gtrsim 2$ (Marchesini et al. 2022), (10) measurements of the rest-frame UV at $7 < z < 9$ (Leethochawalit et al. 2022), (11) masses and M/L at $z > 7$ (Santini et al. 2022), (12) the morphology of high- z galaxies (Treu et al. 2022a), (13) faint cold brown dwarfs (Nonino et al. 2022), (14) a morphological atlas at $1 < z < 5$ (Jacobs et al. 2022), (15) faint high- z sources are intrinsically blue (Glazebrook et al. 2022), (16) UV slopes at $4 < z < 7$ (Nanayakkara et al. 2022), and (17) star-formation histories at $5 < z < 7$ (Dressler et al. 2022).

Other results from the GLASS observations include a lensing model of Abell 2722 (Bergamini et al. 2022) and two studies using ALMA data of $z > 12$ candidates (Bakx et al. 2022; Popping 2022).

3.1.4. DD-ERS 1328; A JWST Study of the Starburst-AGN Connection in Merging LIRGs

Luminous Infrared Galaxies (LIRGs) are some of the most active regions of star formation in the Universe. The connection between starbursts and Active Galactic Nuclei (AGN), and the role of galaxy merging in feeding both the star formation and supermassive black hole growth, has implications for both feedback and the star-formation history of the Universe. Program 1328 (e.g., [Lai et al. 2022](#)) will obtain NIRSpec and MIRI IFU spectroscopy, along with NIRCам and MIRI imaging, of active galaxies taken from the Great Observatories All-Sky LIRG Survey ([Armus et al. 2009](#), GOALS).

Initial results from GOALS-JWST include detection of an AGN-driven outflow from the nucleus of NGC 7469 using mid-IR spectroscopy ([Armus et al. 2022](#)), and a map of the Polycyclic Aromatic Hydrocarbon (PAH), molecular gas emission ([Lai et al. 2022](#)), and ionization states ([U et al. 2022](#)) in the object. NIRCам and MIRI imaging of NGC 7469 show star-forming regions consistent with young (< 5 Myr) stellar populations, showing an age bimodality in the star-forming regions of the ring ([Bohn et al. 2022](#)). GOALS-JWST observations of the merger VV114 resolved its double nuclei and showed that the south-western core had AGN-like colors while the north-eastern core was a starburst ([Evans et al. 2022](#)). About half of the mid-IR emission in the object was diffuse, including PAH emission. Observations of the merging galaxy IIZw096 showed that between 40 at 70 percent of the IR bolometric luminosity came from a single region smaller than 175 pc in radius ([Inami et al. 2022](#)).

3.1.5. *DD-ERS 1334; The Resolved Stellar Populations Early Release Science Program*

The Resolved Stellar Populations DD-ERS program ([Gilbert et al. 2018](#); [Weisz et al. 2023](#)) will observe the globular cluster M92, the ultra-faint dwarf Draco II and the star-forming dwarf WLM to measure the sub-Solar mass stellar initial mass function (IMF), extinction maps, evolved stars, proper motions and globular clusters. The program will use NIRCам imaging with NIRISS imaging in parallel, both using the F090W and F150W filters, with either wide or medium-band filters in the long-wavelength NIRCам channel. The program will also develop point-spread-function-fitting software specific to NIRCам and NIRISS for evaluating crowded stellar populations ([Warfield et al. 2023](#)).

Early results from Program 1334 include color-magnitude diagrams of M92, reaching almost to the bottom of the M92 main sequence ($\sim 0.1M_{\odot}$), and finding white dwarf candidate members of M92 in the brightest portion of the white dwarf cooling sequence ([Nardiello et al. 2022](#)).

3.1.6. *DD-ERS 1335; Q-3D: Imaging Spectroscopy of Quasar Hosts with JWST Analyzed with a Powerful New PSF Decomposition and Spectral Analysis Package*

The Q-3D program uses NIRSpec and MIRI IFU observations of luminous quasars as templates to develop a PSF decomposition and spectral analysis packages, separating the bright central quasar from the host galaxy extended emission ([Wylezalek 2022](#)). The program will measure the stellar, gas and dust components to determine the impact of luminous quasars on their hosts. It will observe three systems: F2M1106, XID2028 and SDSSJ1652.

3.1.7. *DD-ERS 1345; The Cosmic Evolution Early Release Science (CEERS) Survey*

The statistical study of galaxy formation and evolution through deep-field observations with Hubble, Spitzer, Chandra and many other facilities has a rich history, including the Hubble Deep Field ([Williams et al. 1996](#)), the Great Observatories Origins Deep Survey ([Giavalisco et al. 2004](#)), the Hubble Ultra-Deep Field ([Beckwith et al. 2006](#)), The Cosmic Assembly Near-infrared Deep Extragalactic Legacy Survey (CANDELS, [Grogin et al. 2011](#); [Koekemoer et al. 2011](#)), the Frontier Fields ([Lotz et al. 2017](#)) and many others. The CEERS survey will image 100 arcmin² within the CANDELS Extended Groth Strip field with NIRCам and MIRI. The program will obtain NIRSpec MSA and NIRCам WFSS spectroscopy of objects detected in the imaging. The science goals of CEERS includes finding galaxies at $z > 9$ and constraining their nature and abundance, obtaining spectra of galaxies at $z > 3$, including candidates at $z > 6$, and characterizing the MIR emission from galaxies to study dust-obscured star formation and supermassive black hole growth.

Early results from the CEERS data include the discovery of candidate galaxies at $z > 8$ (e.g., [Finkelstein et al. 2022a](#); [Naidu et al. 2022](#); [Topping et al. 2022](#); [Ono et al. 2022](#)), studies of galaxies at $3 < z < 7$, including quiescent galaxies ([Carnall et al. 2022](#)), AGN host galaxies ([Kocevski et al. 2022](#); [Onoue et al. 2022](#); [Ding et al. 2022](#)), star-forming clumps ([Chen et al. 2022c](#)), and sources detected at other wavelengths (e.g., [Chen et al. 2022a](#)).

3.1.8. *DD-ERS 1349; Establishing Extreme Dynamic Range with JWST: Decoding Smoke Signals in the Glare of a Wolf-Rayet Binary*

Colliding-wind Wolf-Rayet (WR) binaries efficiently produce dust, and are important sources for the production of dust in galaxy evolution. WR DustERS ([Lau & WR DustERS Team 2022](#)) will observe two carbon-

rich WR systems; WR-140 is the archetypal colliding-wind binary, while WR-137 is a known periodic dust-maker (Lau et al. 2020). The program will obtain the first resolved mid-infrared spectrum of the dust around a carbon-rich WR star, using MIRI IFU and imaging. They will develop PSF-subtraction techniques for observing faint extended emission around bright sources in IFU datasets. The observations of WR-137 will be done with NIRISS AMI mode to detect the faint dust spiral around the bright central source.

MIRI imaging of WR-140 detected 17 nested dust shells, which formed at each periastron 7.93 years apart over the past 130 years. Understanding the chemical properties and spectral signatures of dust formed by binaries like WR-140 is important given their potential role as dust sources in the inter-stellar medium. MIRI spectroscopy of the second dust shell confirmed the survival of carbonaceous dust grains seen as PAH features, and are consistent with a composition of carbon-rich aromatic compounds in a hydrogen-poor environment. Since this carbonaceous dust has lasted for at least 130 years in the harsh radiation environment of the central binary system, it could be a possible early and potentially dominant source of organic compounds and dust in the ISM of our galaxy (Lau & WR DustERS Team 2022).

3.1.9. *DD-ERS 1355 - TEMPLATES: Targeting Extremely Magnified Panchromatic Lensed Arcs and Their Extended Star formation*

Objects that are magnified by gravitational lensing can be observed with greater intrinsic spatial resolution and higher sensitivity. TEMPLATES (Rigby & Templates Team 2020) will obtain NIRSpec and MIRI IFU spectroscopy and imaging of 4 gravitationally-lensed galaxies selected at $1 < z < 4$. The program will spatially resolve star formation structures in an extinction-robust manner, mapping $H\alpha$, $P\alpha$ and $3.3\mu\text{m}$ PAH features within the galaxies. The selected targets are the brightest and best-characterized lensed systems known.

3.1.10. *DD-ERS 1364 - Nuclear Dynamics of a Nearby Seyfert with NIRSpec Integral Field Spectroscopy*

Measuring the mass of a super-massive black hole in a galaxy can be done with dynamical measurements or with reverberation mapping. It is important to connect dynamical measurements, primarily done on local quiescent galaxies, to reverberation mapping of more distant active galaxies. Program 1364 will use NIRSpec IFU observations of NGC 4151 to directly measure the mass of the central black hole and compare to previous reverberation mapping measurements of the same object (Bentz et al. 2022). The program will measure kinematic maps

of the stars and gas, intensity maps of the gas and stellar dynamical models of the galaxy.

3.1.11. *DD-ERS 1366: The Transiting Exoplanet Community Early Release Science Program*

Transiting exoplanets will allow JWST to measure atmospheric compositions, structures and dynamics in unprecedented detail. Program 1366 will use time-series observations in all four instruments to observe WASP-39b in transit, a MIR phase curve of WASP-43b, and a secondary eclipse of WASP-18b.

Early results include the first clear detection of CO_2 at $4.3\mu\text{m}$ in an exoplanet, WASP-39b (JWST Transiting Exoplanet Community Early Release Science Team et al. 2023). The observations were made with the NIRSpec bright object time sequence mode and the $1.6'' \times 1.6''$ fixed slit aperture. A total of 21,500 integrations over 8.23 hours included the 2.8 hour transit duration.

3.1.12. *DD-ERS 1373: ERS observations of the Jovian System as a demonstration of JWST's capabilities for Solar System science*

JWST enables Solar System observations with moving-target tracking and several modes optimized for bright targets. The pre-launch moving-target tracking requirement was 30 mas/sec, but the telescope managed to track the Double Asteroid Redirection Test (DART) impact on P/Didymos on 2022 September 26 at a rate of 105 mas/sec. Program 1373 is an in-depth study of the Jovian system to characterize Jupiter's cloud layers, winds, composition, auroral activity and temperature structure; to map Io and Ganymede, and to characterize Jupiter's ring structure. The program uses all four instruments.

3.1.13. *DD-ERS 1386: High Contrast Imaging of Exoplanets and Exoplanetary Systems*

The direct characterization of exoplanets with JWST will enable mid-infrared coronagraphy and detailed spectroscopy for the first time. Program 1386 (Hinkley et al. 2022) will use all four instruments to characterize two exoplanets and a circumstellar disk in the NIR and MIR. Early results include NIRCams and MIRI coronagraphic imaging of the super-Jupiter exoplanet HIP 65426b from $2\mu\text{m}$ to $16\mu\text{m}$ (Carter et al. 2022), the first direct detection of an exoplanet at wavelengths longer than $5\mu\text{m}$. The observations are fit by a mass of $7.4 \pm 1.1 M_{Jup}$. Miles et al. (2022) presented the highest fidelity spectrum to date of a planetary-mass object, VHS 1256 b, which is a $< 20 M_{Jup}$, widely separated, young brown dwarf companion. Water, methane, carbon monoxide, carbon dioxide, sodium and potassium were observed in the JWST spectra, indicating disequilibrium chemistry

and clouds. They made a direct detection of silicate clouds for the first time in a planetary-mass companion.

4. MISSION DESIGN

The JWST mission consists of an observatory, a ground system provided by Space Telescope Science Institute and launch services provided by Arianespace under the direction of ESA. The observatory includes all the on-orbit hardware; the prime contractor for the observatory was Northrop Grumman Aerospace Systems (NGAS). The observatory consists of an optical telescope element provided by Ball Aerospace, a spacecraft and sunshield provided by NGAS and an Integrated Science Instrument Module (ISIM) constructed by Goddard Space Flight Center. The ISIM houses the four science instruments and provides them with thermal, electrical, structural, and data handling support.

The Near-Infrared Camera (NIRCam; [Rieke et al. 2022](#), this issue), was built by Lockheed Martin under the direction of Principal Investigator Marcia Rieke of the University of Arizona. All of the near-infrared instruments include detectors from Teledyne Imaging Systems. The Near-Infrared Spectrograph (NIRSpec; [Böker et al. 2023](#), this issue) was built by EADS Astrium under the direction of ESA, and includes a microshutter assembly (MSA) and detector system built by Goddard Space Flight Center. The Near-Infrared Imager and Slitless Spectrograph (NIRISS [Doyon et al. 2023](#), this issue), was built by Honeywell under the direction of CSA. The Fine Guidance System (FGS) is included with the NIRISS and shares the same optical bench. The Mid-Infrared Instrument (MIRI; [Wright et al. 2023](#), this issue) consists of an optical bench assembly built by a consortium of European countries organized by ESA, a cryocooler built by Northrop Grumman under the direction of Jet Propulsion Laboratories and a detector system by JPL and Raytheon Intelligence & Space.

The mission design and its performance is summarized here. Details provided about the telescope are given by [McElwain et al. \(2023\)](#), (this issue), construction, integration, and test of the observatory by [Menzel et al. \(2023\)](#), (this issue), the on-orbit performance measured during commissioning by [Rigby et al. \(2022a\)](#), (this issue), and the on-orbit backgrounds measured during commissioning by [Rigby et al. \(2022b\)](#), (this issue).

4.1. *Launch, Orbit, Deployments, and Commissioning*

The JWST observatory was launched from *Centre Spatial Guyanais* at 12:20 UTC on 2021 December 25 by an Ariane 5 ECA+ rocket. The launch mass was 6161.4kg. The launch provided a near-perfect trajectory. Three mid-course correction (MCC) burns placed

the observatory in an L2 halo orbit, approximately $1.5 \times 10^6 km$ from Earth. The successful launch and MCC burns used less on-board fuel than allocated; the remaining propellant will enable a fuel-limited lifetime of more than 20 years.

Launch was followed by more than 50 major deployments, which were completed successfully enroute to the final orbit. The major deployed systems included the solar panel, the high-gain antenna, the deployed tower assembly, the sunshield, the secondary mirror, an instrument radiator and the primary mirror wings. The sunshield deployment included 140 membrane release mechanisms, 70 hinge assemblies, 8 deployment motors, 400 pulleys, and 90 cables totaling more than 400m. Following the major deployments, which were completed in the first 14 days, the primary mirror segments and secondary mirror were moved off their launch locks.

At the completion of the deployments, the telescope was pointed at HD 84406 ([Gaia Collaboration et al. 2018](#)) to begin the telescope alignment and phasing process. The major steps included (1) Segment Image Identification, (2) Segment Alignment, (3) Image Stacking, (4) Coarse Phasing, (5) Fine Phasing, (6) Telescope Alignment Over Instrument Fields of View, and (7) Iterate Alignment for Final Correction. Following telescope alignment, commissioning of the instruments included activating all instrument systems and commissioning the 17 science instrument modes. The final commissioning tasks included taking the Early Release Observations (ERO). Commissioning was completed by 2022 July 11 and 12 with the release of the EROs.

4.2. *Optical Telescope Element*

The optical telescope element (OTE) consists of a primary mirror made up of 18 hexagonal beryllium primary mirror segment assemblies (PMSAs), a 0.8m convex secondary mirror, and an aft optical assembly subsystem containing a tertiary mirror and a fine steering mirror. All the mirrors are coated with gold. The PMSAs and secondary mirror were aligned and phased on-orbit using actuators that had a total of 132 degrees of freedom. The total collecting area of the primary mirror is $25.4 m^2$, as measured on-orbit using the NIRCam pupil imaging lens. The telescope was designed to be diffraction-limited at $2 \mu m$ wavelength, defined as having a Strehl ratio > 0.8 ([Bely 2003](#)) at the end of a 5-year post-commissioning lifetime, equivalent to 150nm, root-mean squared (RMS) wavefront error (WFE). The WFE at the end of commissioning was ~ 80 nm RMS, equivalent to a diffraction limit at $1.1 \mu m$. The expected degradation of the wavefront error due to micrometeoroid impacts and other effects over the operational life-

time of the mission will be closely monitored (McElwain et al. 2023; Rigby et al. 2022a, this issue).

4.3. *Spacecraft*

The spacecraft provides power, pointing, orbit maintenance, data storage and communications for the observatory. At the end of commissioning, the solar array provided an average of 1.5 kW of power with the ability to provide 3 kW when needed. The pointing system uses star trackers, inertial reference units (IRUs) containing gyros, reaction wheels, and a fine steering mirror (FSM) to point the telescope. There are three star trackers, one of which provides redundancy. There are two IRUs, one of which is redundant; each IRU includes four gyros, one of which provides redundancy. There are six reaction wheels, of which two provide redundancy. The star trackers, gyros and reaction wheels maintain the attitude and coarse pointing of the observatory. During fine guiding, after guide star acquisition, the FGS provides a 16 Hz positional update to the fine steering mirror to adjust the pointing of the telescope. At the end of commissioning, the pointing system delivers pointing stability of $\sim 1mas$ (1σ per axis), greatly exceeding the pre-launch estimates of $\sim 6mas$. Orbit maintenance currently requires firing the on-board thrusters about once every 6 weeks. The thruster firings are also used to maintain angular momentum by de-spinning the reaction wheels. The frequency of orbit maintenance and angular momentum management is determined through ranging measurements and reaction wheel telemetry.

The on-board solid-state recorder holds 471 Gbits of science and engineering data. The data are downlinked via Ka band through the Deep Space Network (DSN) on a nominal schedule of two contacts per day totaling up to 12 hours. The actual downlink schedule varies from day to day with which antenna is in range and DSN scheduling with respect to other mission needs. Commands and observation plans are uplinked to the observatory through the DSN using S band.

4.4. *Sunshield and Cooling*

The sunshield consists of 5 layers of Kapton, about $14m \times 22m$ in size, that separate the $\sim 300K$ spacecraft from the telescope, and attenuate the ~ 200 kW of incident Solar radiation to mW levels. The sunshield size and geometry provides an instantaneous field of regard of 40% of the sky in an annulus that sweeps around the full sky once per year; each point on the sky is visible at least once in each six-month period. The telescope can point 5deg towards the Sun and 45deg away from the Sun, and can spin around the Sun-anti-Sun axis.

Immediately after launch, the observatory began passively cooling, a process that was completed within

120 days. The cooldown was controlled using heaters to ensure that the instruments would not be contaminated by condensation of outgassing water and other volatiles. The MIRI cryocooler (the only active cooling in the observatory) was turned on after the deployments and reached its final temperature on day 104. The final temperature reached by the secondary mirror is 29.2K. The primary mirror segments range from 34.7K to 54.5K, with the mirror segments closest to the core region near the sunshield at the bottom of the telescope warmer than the mirror segments at the top and wings. With these temperatures, JWST broad-band observations are background limited by zodiacal light out to about $12.5\mu m$ wavelength, and limited by thermal self-emission at longer wavelengths (Rigby et al. 2022b, this issue). The near-infrared instrument detector plane temperatures are actively maintained using heaters at 38.5K for NIRC*am* and NIRISS, and 42.8K for NIRSpec. The MIRI optical assembly is kept at 6K by the cryocooler, while the MIRI shield around the instrument is about 20K.

5. INSTRUMENTS

JWST has four science instruments with a total of 17 science instrument modes (see Table 4). All of the instrument capabilities expected before launch have been enabled and are in use. Almost all of the instrument requirements have been exceeded; in particular most of the instrument modes are more sensitive than the pre-launch expectations, and the point spread function at the shorter wavelengths is sharper than the pre-launch expectations.

5.1. *NIRC*am**

NIRC*am* (Rieke et al. 2003; Horner & Rieke 2004; Rieke et al. 2022, this issue) provides imaging from $0.6\mu m$ to $5.0\mu m$ in broad-band, medium-band and narrow-band filters. It has a wide-field slitless spectroscopy capability from $2.5\mu m$ to $5.0\mu m$. It has a coronagraphic mode. NIRC*am* is designed with two modules observing parallel fields of view; each module contains a dichroic at $2.4\mu m$ to provide simultaneous data in two filters longward and shortward of the dichroic. The two modules are identical, including the wavefront sensing hardware, and provide full redundancy in case of failure. The total field of view is $2.2 \times 4.4 arcmin^2$, and there are a total of ten detectors, with 8 in the short wavelength channel and 2 in the long wavelength channel. All of the near-infrared instruments (NIRC*am*, NIRSpec, NIRISS, and FGS) use H2RG HgCdTe 2048×2048 focal-plane arrays made by Teledyne Imaging Systems (e.g., Rauscher

Table 4. Science Instrument Characteristics

| Instrument | Wavelength (μm) | Detector | Plate Scale (mas/pix) | Field of View |
|----------------------|------------------------|--------------------------|-----------------------|--|
| NIRCam | | | | |
| short | 0.6 - 2.3 | Eight 2048 \times 2048 | 32 | 2.2 \times 4.4 arcmin |
| long ^a | 2.4 - 5.0 | Two 2048 \times 2048 | 65 | 2.2 \times 4.4 arcmin |
| NIRSpec | | | | |
| MSA ^b | 0.6 - 5.0 | Two 2048 \times 2048 | 100 | 3.4 \times 3.1 arcmin |
| slits ^c | | | | \sim 200 mas \times 4 arcsec |
| IFU | | | | 3.0 \times 3.0 arcsec |
| MIRI | | | | |
| imaging | 5 - 27 | 1024 \times 1024 | 110 | 1.4 \times 1.9 arcmin |
| spectra ^d | 5 - 10 | | | 26 \times 26 arcsec |
| IFU | 5 - 28 | Two 1024 \times 1024 | 200 to 470 | 3.6 \times 3.6 to 7.5 \times 7.5 arcsec |
| NIRISS | | | | |
| imaging | 0.6 - 5.0 | 2048 \times 2048 | 65 | 2.2 \times 2.2 arcmin |
| WFSS | 0.8 - 2.2 | | | |
| SOSS | 0.6 - 2.8 | | | |
| AMI | 2.8 - 4.8 | | | |
| FGS | | | | |
| | 0.6 - 5.0 | Two 2048 \times 2048 | 65 | 2.2 \times 4.4 arcmin |

NOTE—a) Use of a dichroic renders the NIRCam long-wavelength field of view co-spatial with the short wavelength channel, and the two channels acquire data simultaneously. (b) NIRSpec includes a micro-shutter assembly (MSA) with four 384 \times 175 micro-shutter arrays. The individual shutters are each 250 (spectral) \times 500 (spatial) mas. (c) NIRSpec also includes several fixed slits which provide redundancy and high contrast spectroscopy on individual targets, and an integral field unit (IFU). (d) MIRI includes a fixed slit for low-resolution ($R\sim 100$) spectroscopy over the 5 to 10 μm range, and an integral field unit for $R\sim 3000$ spectroscopy over the full 5 to 28 μm range. The long wavelength cut-off for MIRI spectroscopy is set by the detector performance, which drops beyond 28.0 μm .

et al. 2014). The NIRCam plate scales are 32 milli-arcsec per pixel in the short wavelength channels and 65 milli-arcsec per pixel in the long wavelength channels, Nyquist sampling the diffraction limit at 2.0 μm and 4.0 μm , respectively. NIRCam also functions as part of the wave-front sensing and control system.

5.1.1. NIRCam imaging

NIRCam contains 2 extra-wide filters, 8 broad-band filters, 12 medium-band filters and 7 narrow-band filters. The broad-band filters span the full wavelength range of the instrument, the extra-wide and medium-band filters cover 1.0 μm to 4.0 μm and 1.4 μm to 5.0 μm respectively, and the narrow-band filters are selected to match individual spectral lines. NIRCam imaging sen-

sitivity exceeds the pre-launch expectations in almost all filters. The requirements were 11.4nJy and 13.8nJy at 2.0 μm and 3.5 μm , point-source sensitivity, 10σ in 10,000s. The sensitivity at the end of commissioning were 7.3nJy and 8.8nJy respectively. NIRCam imaging is one of the most-used modes in Cycle 1 programs. An example program that uses this mode is Program 1963, a medium-band survey of the Hubble Ultra Deep Field.

5.1.2. NIRCam wide-field slitless spectroscopy

NIRCam wide-field slitless spectroscopy (WFSS Greene et al. 2017) provides $R \sim 1600$ spectra of all of the objects within the field of view using a grism. The grism is used in the long wavelength channel in combination with a wide or medium filter to provide

spectroscopy in the $2.5\mu\text{m}$ to $5.0\mu\text{m}$ wavelength range. Short wavelength $< 2.5\mu\text{m}$ imaging in the short wavelength channel can be taken simultaneously with the WFSS measurements. Commissioning data show that the total throughput is 20% to 40% higher than pre-launch expectations. An example using this mode is Program 2078, searching for galaxies at the same redshift as $6.5 < z < 6.8$ quasars. Sun et al. (2022a,b) discovered $\text{H}\alpha + [\text{O III}] \lambda 5007$ line emitters at $z > 6$ using the NIRC*Cam* WFSS mode in commissioning data.

5.1.3. NIRC*Cam* coronagraphy

NIRC*Cam* coronagraphy (Krist et al. 2009) has 3 round and two bar-shaped coronagraphic masks for occulting a bright object. The inner working angles range from $0.40''$ to $0.81''$ for the round masks, corresponding to $6\lambda/D$ at $2.1\mu\text{m}$, $3.35\mu\text{m}$ and $4.1\mu\text{m}$, and $0.13''$ to $0.88''$ for the bar masks. During a bar observation, the bright object is positioned behind the bar at the location where the IWA $\sim 4\lambda/D$. The masks are used in conjunction with a filter. Commissioning demonstrated that this mode provided a 5σ contrast at $1''$ better than 4×10^{-5} (Girard et al. 2022). An example using this mode is Program 1386, the DD-ERS high-contrast exoplanet imaging program (Hinkley et al. 2022; Carter et al. 2022).

5.1.4. NIRC*Cam* bright object time series - imaging

Bright object time series (BOTS) observations are designed to measure photometric variations in relatively bright sources. NIRC*Cam* imaging BOTS uses rapid readout of sub-arrays ranging from 64×64 to 160×160 , in combination with filters or a weak lens, to increase the readout cadence and increase the saturation limits. Commissioning observations showed that the NIRC*Cam* BOTS imaging performance was nominal. An example using this mode is Program 2635, studying infrared emission of 4U0142+61, a magnetar with a possible silicate spectral feature at $9.7\mu\text{m}$, which has been interpreted as a passive disk surrounding the energetic isolated neutron star.

5.1.5. NIRC*Cam* bright object time series - grism

NIRC*Cam* grism BOTS observations provide $R \sim 1600$ spectroscopic observations of bright, isolated, time-varying sources. The spectroscopy in the long-wavelength channel is paired with weak lens observations in the short-wavelength channel to avoid saturation. This mode is capable of observing targets as bright as naked-eye stars ($\text{mag} < 5$). Commissioning observations of the transiting exoplanet HAT-P-14 b obtained a 91 ppm spectrum (when binned to $R = 100$). An example using this mode is Program 2084, searching for lava rain on the hot super-Earth planet 55 Cancri e.

5.2. NIRSpec

NIRSpec (Jakobsen et al. 2022; Böker et al. 2023, this issue) provides spectroscopy from 0.6 to $5.3 \mu\text{m}$ at $R \sim 100$, $R \sim 1000$ and $R \sim 3000$ using fixed slits, a microshutter assembly (MSA) (Ferruit et al. 2022), or an integral field unit (IFU) (Böker et al. 2022). The detector system consists of two Teledyne 2048×2048 H2RG arrays controlled and read by SIDECAR ASICs. The $18\mu\text{m} \times 18\mu\text{m}$ pixels of the detector arrays project to an average of $0.103''$ in the dispersion direction and $0.105''$ in the spatial direction. Dispersion is done with a prism ($R = 30 - 300$) or gratings ($R = 500 - 1343$ or $R = 1321 - 3690$). The dispersion is crossed with filters to limit the bandwidth and resulting length of the spectra on the detectors. In most cases, the throughput of the instrument is higher than pre-launch expectations.

5.2.1. NIRSpec multi-object spectroscopy

NIRSpec multi-object spectroscopy is done using the MSA, which is a MEMS assembly consisting of four quadrants. Each MSA slit is $0.203''$ by $0.463''$, with a $\sim 0.07''$ wall between the openings. There are 730 (spectral) by 342 (spatial) pixels in the full array, spanning a field of view of approximately $3.6'$ by $3.4'$. The MSA is fully configurable, except for a limited number of failed slits. Typically, the MSA can be configured to observe up to 100 objects simultaneously, including sky subtraction, without overlapping spectra. Multi-object spectroscopy is one of the most highly used instrument modes in Cycle 1. An example using mode is Program 1345, The Cosmic Evolution Early Release Science (CEERS) Survey, the DD-ERS program targeting a deep field.

5.2.2. NIRSpec fixed slit spectroscopy

NIRSpec has five fixed slits, which provide the highest contrast and throughput on individual targets for NIRSpec. The fixed slits also provide a redundant spectroscopic capability to the mission if the MSA mechanism were to fail. Three fixed slits are $0.2''$ wide by $3.3''$ long, and one is $0.4''$ wide by $3.8''$ long. There is also a $1.6'' \times 1.6''$ high-throughput slit that is primarily used with the NIRSpec bright object time series mode. An example using this mode is Program 1936, a target of opportunity program which will target a kilonova detected by the LIGO/Virgo/KAGRA gravitational wave detectors during their Observing Run 4.

5.2.3. NIRSpec integral field unit spectroscopy

The IFU entrance aperture is a contiguous $3.1'' \times 3.2''$ field of view, divided into 30 slices totaling 900 spaxels, each $0.103'' \times 0.105''$. By providing a full spectral

data cube, the mode gives the most complete information on a single target in the near-infrared with JWST. The throughput is slightly lower than pre-launch expectations in the red, but higher in the blue. An example using this mode is 1355, Targeting Extremely Magnified Panchromatic Lensed Arcs and Their Extended Star formation (TEMPLATES), the DD-ERS program that targets individual galaxies that are highly boosted by gravitational lensing.

5.2.4. *NIRSpec bright object time series*

NIRSpec BOTS (Birkmann et al. 2022) primarily uses the $1.6'' \times 1.6''$ fixed slit, combined with detector subarrays either 16 or 32 pixels wide, to rapidly monitor bright time-varying objects such as observations of stars with transiting exoplanets. The readout cadence can be as fast as 0.28s, potentially reaching stars brighter than $J < 6$ in some modes. During commissioning, the mode was tested on HAT-P-14 b, and reached a noise level of < 60 ppm (Espinoza et al. 2022). An example using this mode in Cycle 1 is Program 2159, following a hot super-Earth-size exoplanet for a full orbit to map the planet’s temperature.

5.3. *NIRISS*

NIRISS (Doyon et al. 2012, 2023, this issue) provides three specialized scientific capabilities and redundant broad-band imaging, over the wavelength range $0.7\mu\text{m}$ to $5.0\mu\text{m}$. NIRISS is packaged with the FGS, which provides the signal to the fine steering mirror and the attitude control system to lock onto targets and provide fine guiding. NIRISS has a field of view of $2.2' \times 2.2'$, matching the FOV of one of the two NIRCcam channels. NIRISS has a single 2048×2048 $5\mu\text{m}$ cut-off Hawaii-2RG detector, with 65 milliarcsec per pixel.

5.3.1. *NIRISS single object slitless spectroscopy*

NIRISS single-object slitless spectroscopy (SOSS) (Albert et al., in prep) defocuses the telescope beam to spread the signal from bright objects over about 25 pixels to avoid saturation. SOSS provides medium-resolution spectroscopy ($R \sim 70$) between $0.6\mu\text{m}$ and $2.8\mu\text{m}$. There are two usable orders. Using subarrays shortward of $1.0\mu\text{m}$ allows targets as bright as $J = 6.5$ (Vega mag). An example is Program 2589, where the SOSS mode will be used to detect and characterize the possible atmospheres of the small, rocky exoplanets TRAPPIST 1b and 1c.

5.3.2. *NIRISS wide field slitless spectroscopy*

NIRISS wide-field slitless spectroscopy (WFSS) (Willott et al. 2022) enables low-resolution ($R \sim 150$)

slitless spectroscopy over the $2.2' \times 2.2'$ FOV at $0.8\mu\text{m}$ to $2.2\mu\text{m}$ wavelength. It is optimized to search for Ly- α emitting galaxies during the epoch of reionization. It can also be used efficiently in parallel mode. Two orthogonal gratings provide dispersion in two directions to disentangle overlapping spectra and reduce confusion in crowded fields. The gratings are crossed with wide- or medium-band filters, which also reduces blending of the objects. Throughput of the WFSS mode exceeds the pre-launch expectations. An example is Program 1571, PASSAGE – Parallel Application of Slitless Spectroscopy to Analyze Galaxy Evolution, a pure-parallel search for active star-forming galaxies.

5.3.3. *NIRISS aperture masking interferometry*

NIRISS aperture masking interferometry (AMI, Sivaramakrishnan et al. 2012, 2022) uses a seven-aperture mask to enable high-contrast imaging at an inner working angles less than λ/D . AMI is used with the F380M, F430M, or F480M filters, and typically uses an 80×80 pixel subarray for bright sources. During commissioning, AMI was demonstrated by detecting AB Dor C, a companion separated by $\sim 0.3''$ with a contrast ratio of 4.5 mag (Kammerer et al. 2022). An example is the DD-ERS Program 1349, WR DustERS, which will observe the Wolf-Rayet binary WR 137 with AMI to investigate the dust abundance, composition, and production rates of dusty sources in the colliding winds of the stars.

5.3.4. *NIRISS imaging*

NIRISS includes an imaging capability using a set of backup NIRCcam broad-band filters and some medium-band filters. As NIRISS imaging covers half the FOV of NIRCcam, and does not include a dichroic, this mode is primarily for imaging redundancy in the mission. NIRISS imaging can also be used in parallel to NIRCcam imaging for additional areal coverage, and is used in support of WFSS data. Program 2561, which will observe the Frontier Field lensing cluster Abell 2744, uses NIRISS imaging in parallel to NIRCcam imaging to increase the area of deep photometric studies of high-redshift galaxies at mild lensing magnifications.

5.4. *MIRI*

MIRI (Rieke et al. 2015a; Wright et al. 2015, 2023, this issue) provides both imaging in broad-band filters and IFU spectroscopy from $5.0\mu\text{m}$ to $28.0\mu\text{m}$. It also has low-resolution slit spectroscopy from $5.0\mu\text{m}$ to $12.0\mu\text{m}$ (where the sensitivity is limited by the zodiacal light background) and a coronagraphic capability. MIRI has three arsenic-doped silicon (SI:As) impurity band conduction detector arrays, each of 1024×1024 pixel format

with $25\mu\text{m}$ pixel pitch, made by Raytheon Intelligence & Space (Ressler et al. 2015; Rieke et al. 2015b). The plate scale is 110 milli-arcsec per pixel, which Nyquist samples the point spread function at $6.25\mu\text{m}$. Two of the detectors are used for the medium-resolution spectroscopy, while the third is used for imaging, low-resolution spectroscopy and coronagraphy. The MIRI instrument is actively cooled to an operating temperature of 6.0K with a $\sim 6\text{K}/18\text{K}$ hybrid mechanical cooler, developed by Northrop Grumman in collaboration with JPL. The MIRI cooler uses gaseous helium as the coolant. There is a three stage Pulse-Tube Precooler which reaches $\sim 18\text{K}$ and a fourth $\sim 6\text{K}$ Joule-Thompson cooler stage. The cooler compressor is in the JWST spacecraft bus at room temperature, while the cold head assembly cooling the instrument is on the ISIM structure.

5.4.1. *MIRI imaging*

MIRI imaging (Bouchet et al. 2015) uses 9 broad-band filters to cover the $5\mu\text{m}$ to $27\mu\text{m}$ wavelength region. The imaging field of view is $1.4 \times 1.9\text{arcmin}^2$ sampled with $0.11''$ pixels. (The remaining field of view of the detector is occupied by the coronagraphs and the low-resolution spectrometer.) MIRI imaging can use sub-array readouts for bright objects that would saturate in a full frame, observing objects as bright as $0.1Jy$ in the F560W filter (Glasse et al. 2015). An example using this mode is Program 2130, which will observe several square kpc in three nearby galaxies, M33, NGC 300 and NGC 7793, to measure dust-enshrouded stellar populations.

5.4.2. *MIRI low-resolution spectroscopy*

MIRI low-resolution spectroscopy (LRS Kendrew et al. 2015) provides $R \sim 100$ long-slit and slitless spectroscopy from $5\mu\text{m}$ to $12\mu\text{m}$, the MIR wavelength range where JWST observations are still zodiacal-light limited. A slit mask is permanently in the field of view; slitless spectroscopy is available anywhere within the imager field of view when the $R \sim 100$ double prism assembly is selected in the imaging filter wheel. For bright sources, a sub-array readout can be used. In practice, the source will be placed in a dedicated LRS slitless detector region and read out in a sub-array. It is expected that most LRS slitless targets will be bright nearby stars with transiting planets to obtain spectra of exoplanet atmospheres. Program 1658 will observe Pluto’s moon Charon using the MIRI LRS mode.

5.4.3. *MIRI medium-resolution spectroscopy*

MIRI medium-resolution spectroscopy (MRS Wells et al. 2015) provides integral-field spectroscopy over the full $5\mu\text{m}$ to $28\mu\text{m}$ MIRI wavelength range. The spectral resolution ranges from ~ 3300 at the short wave-

length end to ~ 1300 at the longest wavelengths. There are four channels separated in wavelength by dichroics, with between 12 and 21 image slices. Depending on wavelength, the field of view ranges from $3.70'' \times 3.70''$ to $7.74'' \times 7.95''$. Each individual exposure provides two wavelength ranges on two detectors; three exposures are required to get a full wavelength spectrum. MIRI MRS is used in many programs; an example is Program 1549 which will observe three molecule-rich protoplanetary disks that were shown to have very bright water line emission in Spitzer spectra.

5.4.4. *MIRI coronagraphic imaging*

The imaging channel on MIRI includes four coronagraphs (Boccaletti et al. 2015) for high-contrast imaging. The four coronagraphs are optimized for observations at $10.65\mu\text{m}$, $11.40\mu\text{m}$, $15.50\mu\text{m}$ and $\sim 23\mu\text{m}$. The short wavelength coronagraphs use four-quadrant phase masks (4QPM; Rouan et al. 2000, 2007), while the other is a more traditional Lyot design with an occulting spot in the image plane and a stop in the pupil plane. The 4QPMs are usable at a smaller inner working angle than more traditional designs, and can reach near $1\lambda/D$. Each of the 4QPMs provides a field of $24'' \times 24''$, while the Lyot spot mask provides $30'' \times 30''$ field of view. Each of the coronagraphs demonstrated a raw contrast ratio $> 10,000$ at $6\lambda/D$ during commissioning. An example using this mode is Program 1618, which will search for planets and zodiacal dust around Alpha Centauri A.

6. SCIENCE OPERATIONS AND PROPOSAL PREPARATION

JWST is controlled from a Mission Operations Center (MOC) at the Space Telescope Science Institute (STScI), which also runs the JWST science program. STScI issues annual calls for proposals (CFPs) for the General Observer programs. In between the CFPs, proposals for time-critical observations, or other observations that cannot be proposed to the annual call are considered for the Director’s Discretionary time. The scope of JWST’s competitively-selected programs range from large and Treasury programs that address multiple science goals and produce multi-use datasets to small programs that target important but specific science goals. All of the JWST data taken, including science programs and calibration data, are placed in the Mikulski Archive for Space Telescopes (MAST) at STScI and made available to the original proposers within a day or two of the data being taken. After an exclusive use period that ranges from 0 to 12 months depending on the type of program, the data are also freely available to other astronomers for archival research and other purposes.

In response to the annual CFP, proposals are prepared using the Astronomer’s Proposal Tool (APT) software package, which allows the proposer to specify both the textual proposal information (e.g., Title, Abstract, investigators, etc.) and the specifics of the observations. The APT is a sophisticated software package that ensures appropriate selection of observing parameters, checks the feasibility of the observations, and determines the times of the year that the observations could be scheduled, including planning guide star availability. APT also calculates the total allocated time needed for the observations. The text of the scientific justification and other proposal sections are attached to the proposal as a PDF within APT.

In addition to APT, observers will use the JWST Exposure Time Calculator (ETC) to determine many of the observation parameters, and to ensure that the observations reach the depth required for the science. The APT and ETC together contain sophisticated data simulation tools to visualize potential JWST observations. APT and the ETC are documented in an extensive series of on-line pages known as the JWST User Documentation (JDox, [STScI 2016](#))¹. JDox also documents the JWST data analysis tools.

7. GETTING JWST TO SPACE, WHAT MIGHT WE FIND, AND WHAT’S NEXT?

Building on the inspiring and poetic 1996 HST and Beyond report of the Dressler committee, and with the vigorous support of NASA, ESA, and CSA leadership, the JWST team settled on the four top scientific priorities, documented the instrument and telescope performance requirements to meet scientific objectives, made plans, matured 10 technologies, made international agreements, and chose the instrument teams and contractors. The result is the world’s most powerful space telescope, performing better than expectations, with a projected lifetime of 20 years. We have reviewed the history, key technical choices, and we celebrate the people who made the observatory real.

We already see progress in the four key science themes. JWST has begun to address questions of the first galaxies and reionization by measuring spectroscopic redshifts of metal-poor galaxies beyond $z > 13$ ([Curtis-Lake et al. 2022](#)), detecting multiple emission lines in a galaxy at $z = 10.6$ ([Bunker et al. 2023](#)), and measuring galaxy

luminosity functions at $z > 7$ ([Finkelstein et al. 2022b](#)). JWST has studied galaxy assembly by detecting galaxy bars at $z > 1$ ([Guo et al. 2023](#)) and examining the quasar-galaxy connection at $z = 2.94$ ([Wylezalek 2022](#)). JWST has peered into star-forming regions to study the interactions between massive stars and the surrounding material ([Reiter et al. 2022](#)) and measured the ice chemistry in a prestellar cloud ([McClure et al. 2023](#)). JWST has measured the temperature of a rocky exoplanet ([Greene et al. 2023](#)), and made the first detection of CO₂ in an exoplanet atmosphere ([JWST Transiting Exoplanet Community Early Release Science Team et al. 2023](#)). JWST observed the impact of NASA’s Double Asteroid Redirection Test (DART) into asteroid Dimorphos and has made a detailed study of the Jovian system ([de Pater et al. 2022](#)). Further JWST observations will continue to address the original science themes, and it is likely that the universe will surprise us with unexpected discoveries. Looking toward the future, our international teams have proven that extremely complex scientific space missions can be successful, paving the way towards the future great observatories recommended by the 2020 Decadal Survey.

8. ACKNOWLEDGMENTS

The JWST mission is a joint project between the National Aeronautics and Space Agency, European Space Agency, and the Canadian Space Agency. The JWST mission development was led at NASA’s Goddard Space Flight Center with a distributed team across Northrop Grumman Corporation, Ball Aerospace, L3Harris Technologies, the Space Telescope Science Institute, and hundreds of other companies and institutions. This mission was created by a team of people whose creativity and dedication made this scientific dream a reality.

Technical contributions were carried out at the Jet Propulsion Laboratory, California Institute of Technology, under a contract with the National Aeronautics and Space Administration (80NM0018D0004).

This work is based on observations made with the NASA/ESA/CSA James Webb Space Telescope. The data were obtained from the Mikulski Archive for Space Telescopes at the Space Telescope Science Institute, which is operated by the Association of Universities for Research in Astronomy, Inc., under NASA contract NAS 5-03127 for JWST.

REFERENCES

¹ For more information about proposing for JWST observing time or archival funding, see: <https://jwst-docs.stsci.edu/>

- Armus, L., Mazzarella, J. M., Evans, A. S., et al. 2009, *PASP*, 121, 559
- Armus, L., Lai, T., U, V., et al. 2022, arXiv e-prints, arXiv:2209.13125
- Bahcall, J., & Astronomy and Astrophysics Survey Committee. 1991, *The Decade of Discovery in Astronomy and Astrophysics*.
- Bakx, T. J. L. C., Zavala, J. A., Mitsuhashi, I., et al. 2022, arXiv e-prints, arXiv:2208.13642
- Beckwith, S. V. W., Stiavelli, M., Koekemoer, A. M., et al. 2006, *AJ*, 132, 1729
- Bely, P. Y. 2003, *The Design and Construction of Large Optical Telescopes*
- Bely, P. Y., Burrows, C. J., & Illingworth, G. D. 1990, *The Next Generation Space Telescope*
- Bentz, M. C., Williams, P. R., & Treu, T. 2022, *ApJ*, 934, 168
- Bergamini, P., Acebron, A., Grillo, C., et al. 2022, arXiv e-prints, arXiv:2207.09416
- Berné, O., Habart, É., Peeters, E., et al. 2022, *PASP*, 134, 054301
- Birkmann, S. M., Ferruit, P., Giardino, G., et al. 2022, *A&A*, 661, A83
- Boccaletti, A., Lagage, P. O., Baudoz, P., et al. 2015, *PASP*, 127, 633
- Bohn, T., Inami, H., Diaz-Santos, T., et al. 2022, arXiv e-prints, arXiv:2209.04466
- Böker, T., Arribas, S., Lützgendorf, N., et al. 2022, *A&A*, 661, A82
- Böker, T., Beck, T. L., Birkmann, S. M., et al. 2023, arXiv e-prints, arXiv:2301.13766
- Bouchet, P., García-Marín, M., Lagage, P. O., et al. 2015, *PASP*, 127, 612
- Boyett, K., Mascia, S., Pentericci, L., et al. 2022, arXiv e-prints, arXiv:2207.13459
- Bunker, A. J., Saxena, A., Cameron, A. J., et al. 2023, arXiv e-prints, arXiv:2302.07256
- Burrows, C. J., Holtzman, J. A., Faber, S. M., et al. 1991, *ApJL*, 369, L21
- Carnall, A. C., McLeod, D. J., McLure, R. J., et al. 2022, arXiv e-prints, arXiv:2208.00986
- Carter, A. L., Hinkley, S., Kammerer, J., et al. 2022, arXiv e-prints, arXiv:2208.14990
- Castellano, M., Fontana, A., Treu, T., et al. 2022, *ApJL*, 938, L15
- Chen, C.-C., Gao, Z.-K., Hsu, Q.-N., et al. 2022a, *ApJL*, 939, L7
- Chen, W., Kelly, P. L., Treu, T., et al. 2022b, arXiv e-prints, arXiv:2207.11658
- Chen, Z., Stark, D. P., Endsley, R., et al. 2022c, arXiv e-prints, arXiv:2207.12657
- Curtis-Lake, E., Carniani, S., Cameron, A., et al. 2022, arXiv e-prints, arXiv:2212.04568
- de Pater, I., Fouchet, T., Wong, M., et al. 2022, in *AAS/Division for Planetary Sciences Meeting Abstracts*, Vol. 54, AAS/Division for Planetary Sciences Meeting Abstracts, 306.07
- Ding, X., Silverman, J. D., & Onoue, M. 2022, arXiv e-prints, arXiv:2209.03359
- Doyon, R., Willott, C. J., Hutchings, J., et al. 2023, *PASP*, submitted
- Doyon, R., Hutchings, J. B., Beaulieu, M., et al. 2012, in *Society of Photo-Optical Instrumentation Engineers (SPIE) Conference Series*, Vol. 8442, *Space Telescopes and Instrumentation 2012: Optical, Infrared, and Millimeter Wave*, ed. M. C. Clampin, G. G. Fazio, H. A. MacEwen, & J. Oschmann, Jacobus M., 84422R
- Dressler, A., & HST and Beyond Committee. 1996, *HST and beyond.*, Association of Universities for Research in Astronomy, 1996, xiv, p. 89, Washington, D.C.
- Dressler, A., Vulcani, B., Treu, T., et al. 2022, arXiv e-prints, arXiv:2208.04292
- Espinoza, N., Úbeda, L., Birkmann, S. M., et al. 2022, arXiv e-prints, arXiv:2211.01459
- Evans, A. S., Frayer, D., Charmandaris, V., et al. 2022, arXiv e-prints, arXiv:2208.14507
- Feinberg, L. D., Clampin, M., Keski-Kuha, R., et al. 2012, in *Society of Photo-Optical Instrumentation Engineers (SPIE) Conference Series*, Vol. 8442, *Space Telescopes and Instrumentation 2012: Optical, Infrared, and Millimeter Wave*, ed. M. C. Clampin, G. G. Fazio, H. A. MacEwen, & J. Oschmann, Jacobus M., 84422B
- Ferruit, P., Jakobsen, P., Giardino, G., et al. 2022, *A&A*, 661, A81
- Field, G. B., & Astronomy and Astrophysics Survey Committee. 1983, in *Washington*, Vol. 1, 1
- Fienup, J. R., Marron, J. C., Schulz, T. J., & Seldin, J. H. 1993, *ApOpt*, 32, 1747
- Finkelstein, S. L., Bagley, M. B., Arrabal Haro, P., et al. 2022a, arXiv e-prints, arXiv:2207.12474
- Finkelstein, S. L., Bagley, M. B., Ferguson, H. C., et al. 2022b, arXiv e-prints, arXiv:2211.05792
- Freedman, W. L., Madore, B. F., Gibson, B. K., et al. 2001, *ApJ*, 553, 47
- Gaia Collaboration, Brown, A. G. A., Vallenari, A., et al. 2018, *A&A*, 616, A1
- Gardner, J. P., Cowie, L. L., & Wainscoat, R. J. 1993, *ApJL*, 415, L9
- Gardner, J. P., & Satyapal, S. 2000, *AJ*, 119, 2589

- Gardner, J. P., Mather, J. C., Clampin, M., et al. 2006, *SSRv*, 123, 485
- Giavalisco, M., Ferguson, H. C., Koekemoer, A. M., et al. 2004, *ApJL*, 600, L93
- Gilbert, K., Weisz, D., & Resolved Stellar Populations ERS Program Team. 2018, in *American Astronomical Society Meeting Abstracts*, Vol. 232, *American Astronomical Society Meeting Abstracts #232*, 210.02
- Girard, J. H., Leisenring, J., Kammerer, J., et al. 2022, in *Society of Photo-Optical Instrumentation Engineers (SPIE) Conference Series*, Vol. 12180, *Space Telescopes and Instrumentation 2022: Optical, Infrared, and Millimeter Wave*, ed. L. E. Coyle, S. Matsuura, & M. D. Perrin, 121803Q
- Glasse, A., Rieke, G. H., Bauwens, E., et al. 2015, *PASP*, 127, 686
- Glazebrook, K., Nanayakkara, T., Jacobs, C., et al. 2022, *arXiv e-prints*, arXiv:2208.03468
- Greene, T. P., Bell, T. J., Ducrot, E., et al. 2023, *arXiv e-prints*, arXiv:2303.14849
- Greene, T. P., Kelly, D. M., Stansberry, J., et al. 2017, *Journal of Astronomical Telescopes, Instruments, and Systems*, 3, 035001
- Greenhouse, M. 2019, in *2019 IEEE Aerospace Conference*
- Grogin, N. A., Kocevski, D. D., Faber, S. M., et al. 2011, *ApJS*, 197, 35
- Guo, Y., Jogee, S., Finkelstein, S. L., et al. 2023, *ApJL*, 945, L10
- Hinkley, S., Carter, A. L., Ray, S., et al. 2022, *PASP*, 134, 095003
- Horner, S. D., & Rieke, M. J. 2004, in *Society of Photo-Optical Instrumentation Engineers (SPIE) Conference Series*, Vol. 5487, *Optical, Infrared, and Millimeter Space Telescopes*, ed. J. C. Mather, 628–634
- Illingworth, G. 1991, in *JPL D-8541*, Vol. 4, *Technologies for Large Filled Aperture Telescopes in Space*
- Inami, H., Surace, J., Armus, L., et al. 2022, *arXiv e-prints*, arXiv:2208.10647
- Jacobs, C., Glazebrook, K., Calabrò, A., et al. 2022, *arXiv e-prints*, arXiv:2208.06516
- Jakobsen, P., Ferruit, P., Alves de Oliveira, C., et al. 2022, *A&A*, 661, A80
- JWST Transiting Exoplanet Community Early Release Science Team, Ahrer, E.-M., Alderson, L., et al. 2023, *Nature*, 614, 649
- Kaldeich-Schürmann, B. 1998, *ESA Special Publication*, Vol. 429, *The Next Generation Space Telescope: Science Drivers and Technological Challenges*
- Kammerer, J., Girard, J., Carter, A. L., et al. 2022, in *Society of Photo-Optical Instrumentation Engineers (SPIE) Conference Series*, Vol. 12180, *Space Telescopes and Instrumentation 2022: Optical, Infrared, and Millimeter Wave*, ed. L. E. Coyle, S. Matsuura, & M. D. Perrin, 121803N
- Kendrew, S., Scheithauer, S., Bouchet, P., et al. 2015, *PASP*, 127, 623
- Kimble, R. A., Vila, M. B., Van Campen, J. M., et al. 2016, in *Society of Photo-Optical Instrumentation Engineers (SPIE) Conference Series*, Vol. 9904, *Space Telescopes and Instrumentation 2016: Optical, Infrared, and Millimeter Wave*, ed. H. A. MacEwen, G. G. Fazio, M. Lystrup, N. Batalha, N. Siegler, & E. C. Tong, 990408
- Kimble, R. A., Feinberg, L. D., Voyton, M. F., et al. 2018, in *Society of Photo-Optical Instrumentation Engineers (SPIE) Conference Series*, Vol. 10698, *Space Telescopes and Instrumentation 2018: Optical, Infrared, and Millimeter Wave*, ed. M. Lystrup, H. A. MacEwen, G. G. Fazio, N. Batalha, N. Siegler, & E. C. Tong, 1069805
- Kocevski, D. D., Barro, G., McGrath, E. J., et al. 2022, *arXiv e-prints*, arXiv:2208.14480
- Koekemoer, A. M., Faber, S. M., Ferguson, H. C., et al. 2011, *ApJS*, 197, 36
- Krist, J. E., & Burrows, C. J. 1995, *ApOpt*, 34, 4951
- Krist, J. E., Balasubramanian, K., Beichman, C. A., et al. 2009, in *Society of Photo-Optical Instrumentation Engineers (SPIE) Conference Series*, Vol. 7440, *Techniques and Instrumentation for Detection of Exoplanets IV*, ed. S. B. Shaklan, 74400W
- Lai, T. S.-Y., Finnerty, L., Armus, L., et al. 2022, in *American Astronomical Society Meeting Abstracts*, Vol. 54, *American Astronomical Society Meeting Abstracts*, 241.42
- Lambricht, W. H. 1995, *Powering Apollo: James E. Webb of NASA*
- Lau, R. M., Eldridge, J. J., Hankins, M. J., et al. 2020, *ApJ*, 898, 74
- Lau, R. M., & WR DustERS Team. 2022, in *IR2022: An Infrared Bright Future for Ground-based IR Observatories in the Era of JWST.*, 1
- Leethochawalit, N., Trenti, M., Santini, P., et al. 2022, *arXiv e-prints*, arXiv:2207.11135
- Levenson, N. A., & Sembach, K. 2018, in *American Astronomical Society Meeting Abstracts*, Vol. 232, *American Astronomical Society Meeting Abstracts #232*, 202.01
- Lotz, J. M., Koekemoer, A., Coe, D., et al. 2017, *ApJ*, 837, 97

- MacKenty, J. W., & Stiavelli, M. 2000, in *Astronomical Society of the Pacific Conference Series*, Vol. 195, *Imaging the Universe in Three Dimensions*, ed. W. van Breugel & J. Bland-Hawthorn, 443
- Marchesini, D., Brammer, G., Morishita, T., et al. 2022, arXiv e-prints, arXiv:2207.13625
- Mather, J. C., & Stockman, H. S. 2000, in *Society of Photo-Optical Instrumentation Engineers (SPIE) Conference Series*, Vol. 4013, *UV, Optical, and IR Space Telescopes and Instruments*, ed. J. B. Breckinridge & P. Jakobsen, 2–16
- Mather, J. C., Cheng, E. S., Cottingham, D. A., et al. 1994, *ApJ*, 420, 439
- McClure, M. 2022, in 44th COSPAR Scientific Assembly. Held 16-24 July, Vol. 44, 2798
- McClure, M. K., Boogert, A., Linnartz, H., et al. 2018, in *American Astronomical Society Meeting Abstracts*, Vol. 232, *American Astronomical Society Meeting Abstracts #232*, 302.03
- McClure, M. K., Rocha, W. R. M., Pontoppidan, K. M., et al. 2023, *Nature Astronomy*
- McElwain, M. W., Feinberg, L. D., Perrin, M. D., et al. 2023, arXiv e-prints, arXiv:2301.01779
- McKee, C. F., Taylor, J. H., & Astronomy and Astrophysics Survey Committee. 2001, *Astronomy and Astrophysics in the New Millennium*
- Menzel, M., Davis, M., Parrish, K., et al. 2023, *PASP*, submitted
- Merlin, E., Bonchi, A., Paris, D., et al. 2022, *ApJL*, 938, L14
- Miles, B. E., Biller, B. A., Patapis, P., et al. 2022, arXiv e-prints, arXiv:2209.00620
- Moseley, S. H., Fettig, R. K., Kutyrev, A. S., et al. 1999, in *Society of Photo-Optical Instrumentation Engineers (SPIE) Conference Series*, Vol. 3878, *Miniaturized Systems with Micro-Optics and MEMS*, ed. M. E. Motamedi & R. Goering, 392–397
- Naidu, R. P., Oesch, P. A., van Dokkum, P., et al. 2022, arXiv e-prints, arXiv:2207.09434
- Nanayakkara, T., Glazebrook, K., Jacobs, C., et al. 2022, arXiv e-prints, arXiv:2207.13860
- Nardiello, D., Bedin, L. R., Burgasser, A., et al. 2022, *MNRAS*
- National Academies of Sciences, E., & Medicine. 2021, *Pathways to Discovery in Astronomy and Astrophysics for the 2020s*
- Nonino, M., Glazebrook, K., Burgasser, A. J., et al. 2022, arXiv e-prints, arXiv:2207.14802
- Ono, Y., Harikane, Y., Ouchi, M., et al. 2022, arXiv e-prints, arXiv:2208.13582
- Onoue, M., Inayoshi, K., Ding, X., et al. 2022, arXiv e-prints, arXiv:2209.07325
- Perlmutter, S., Aldering, G., Goldhaber, G., et al. 1999, *ApJ*, 517, 565
- Pontoppidan, K. M., Barrientes, J., Blome, C., et al. 2022, *ApJL*, 936, L14
- Popping, G. 2022, arXiv e-prints, arXiv:2208.13072
- Rauscher, B. J. 2014, in *American Astronomical Society Meeting Abstracts*, Vol. 223, *American Astronomical Society Meeting Abstracts #223*, 149.39
- Rauscher, B. J., Boehm, N., Cagiano, S., et al. 2014, *PASP*, 126, 739
- Reiter, M., Morse, J. A., Smith, N., et al. 2022, *MNRAS*, 517, 5382
- Ressler, M. E., Sukhatme, K. G., Franklin, B. R., et al. 2015, *PASP*, 127, 675
- Rieke, G. H., Wright, G. S., Böker, T., et al. 2015a, *PASP*, 127, 584
- Rieke, G. H., Ressler, M. E., Morrison, J. E., et al. 2015b, *PASP*, 127, 665
- Rieke, M. J., Baum, S. A., Beichman, C. A., et al. 2003, in *Society of Photo-Optical Instrumentation Engineers (SPIE) Conference Series*, Vol. 4850, *IR Space Telescopes and Instruments*, ed. J. C. Mather, 478–485
- Rieke, M. J., Kelly, D. M., Misselt, K., et al. 2022, arXiv e-prints, arXiv:2212.12069
- Riess, A. G., Filippenko, A. V., Challis, P., et al. 1998, *AJ*, 116, 1009
- Rigby, J., & Templates Team. 2020, in *American Astronomical Society Meeting Abstracts*, Vol. 235, *American Astronomical Society Meeting Abstracts #235*, 208.12
- Rigby, J., Perrin, M., McElwain, M., et al. 2022a, arXiv e-prints, arXiv:2207.05632
- Rigby, J. R., Lightsey, P. A., García Marín, M., et al. 2022b, arXiv e-prints, arXiv:2211.09890
- Roberts-Borsani, G., Morishita, T., Treu, T., et al. 2022, *ApJL*, 938, L13
- Rouan, D., Baudrand, J., Boccaletti, A., et al. 2007, *Comptes Rendus Physique*, 8, 298
- Rouan, D., Riaud, P., Boccaletti, A., Clénet, Y., & Labeyrie, A. 2000, *PASP*, 112, 1479
- Santini, P., Fontana, A., Castellano, M., et al. 2022, arXiv e-prints, arXiv:2207.11379
- Schmidt, B. P., Suntzeff, N. B., Phillips, M. M., et al. 1998, *ApJ*, 507, 46

- Sivaramakrishnan, A., Lafrenière, D., Ford, K. E. S., et al. 2012, in *Society of Photo-Optical Instrumentation Engineers (SPIE) Conference Series*, Vol. 8442, *Space Telescopes and Instrumentation 2012: Optical, Infrared, and Millimeter Wave*, ed. M. C. Clampin, G. G. Fazio, H. A. MacEwen, & J. Oschmann, Jacobus M., 84422S
- Sivaramakrishnan, A., Tuthill, P., Lloyd, J. P., et al. 2022, arXiv e-prints, arXiv:2210.17434
- Smith, E. P., & Koratkar, A. 1998, *Astronomical Society of the Pacific Conference Series*, Vol. 133, *Science With The NGST (Next Generation of Space Telescope)*
- Smith, E. P., & Long, K. S. 2000, *Astronomical Society of the Pacific Conference Series*, Vol. 207, *Next Generation Space Telescope Science and Technology*
- Stahl, H. P., Feinberg, L. D., & Texter, S. C. 2004, in *Society of Photo-Optical Instrumentation Engineers (SPIE) Conference Series*, Vol. 5487, *Optical, Infrared, and Millimeter Space Telescopes*, ed. J. C. Mather, 818–824
- Stockman, H. S. 1997, *The Next Generation Space Telescope. Visiting a time when galaxies were young.*
- Stockman, H. S., & Mather, J. C. 2001, in *The Extragalactic Infrared Background and its Cosmological Implications*, ed. M. Harwit & M. G. Hauser, Vol. 204, 467
- STScI. 2016, *JWST User Documentation (JDox), JWST User Documentation Website*
- Sun, F., Egami, E., Pirzkal, N., et al. 2022a, *ApJL*, 936, L8
- . 2022b, arXiv e-prints, arXiv:2209.03374
- Thronson, H. A., Hawarden, T. G., Davies, J. K., et al. 1996, *Advances in Space Research*, 18, 171
- Topping, M. W., Stark, D. P., Endsley, R., et al. 2022, arXiv e-prints, arXiv:2208.01610
- Treu, T., Calabro, A., Castellano, M., et al. 2022a, arXiv e-prints, arXiv:2207.13527
- Treu, T., Roberts-Borsani, G., Bradac, M., et al. 2022b, *ApJ*, 935, 110
- U, V., Lai, T., Bianchin, M., et al. 2022, arXiv e-prints, arXiv:2209.01210
- Vanzella, E., Castellano, M., Bergamini, P., et al. 2022, arXiv e-prints, arXiv:2208.00520
- Wade, L. A., Lilienthal, G. W., Terebey, S., et al. 1996, in *Society of Photo-Optical Instrumentation Engineers (SPIE) Conference Series*, Vol. 2807, *Space Telescopes and Instruments IV*, ed. P. Y. Bely & J. B. Breckinridge, 20–31
- Wang, X., Jones, T., Vulcani, B., et al. 2022, *ApJL*, 938, L16
- Warfield, J. T., Richstein, H., Kallivayalil, N., et al. 2023, arXiv e-prints, arXiv:2301.07218
- Weisz, D. R., McQuinn, K. B. W., Savino, A., et al. 2023, arXiv e-prints, arXiv:2301.04659
- Wells, M., Pel, J. W., Glasse, A., et al. 2015, *PASP*, 127, 646
- Werner, M. W., Roellig, T. L., Low, F. J., et al. 2004, *ApJS*, 154, 1
- Williams, R. E., Blacker, B., Dickinson, M., et al. 1996, *AJ*, 112, 1335
- Willott, C. J., Doyon, R., Albert, L., et al. 2022, *PASP*, 134, 025002
- Wright, G., Rieke, G., Glasse, A., et al. 2023, *PASP*, submitted
- Wright, G. S., Wright, D., Goodson, G. B., et al. 2015, *PASP*, 127, 595
- Wylezalek, D. 2022, in *Multiphase AGN Feeding & Feedback II*, 75
- Yang, L., Morishita, T., Leethochawalit, N., et al. 2022, *ApJL*, 938, L17